

JGR Atmospheres

RESEARCH ARTICLE

10.1029/2021JD035342

Key Points:

- Vehicular exhaust, episodes of biomass burning, industrial plumes and aged air strongly influenced the concentration and composition of VOCs
- Higher enhancements of OVOCs in photochemically aged air masses reveal their significant secondary productions at the suburban site
- The estimated biogenic contributions to ambient air isoprene for the suburban site were higher than those for the urban site

Supporting Information:

Supporting Information may be found in the online version of this article.

Correspondence to:

L. K. Sahu and S. N. Tripathi,
lokesah@prl.res.in;
snt@iitk.ac.in

Citation:

Tripathi, N., Sahu, L. K., Wang, L., Vats, P., Soni, M., Kumar, P., et al. (2022). Characteristics of VOC composition at urban and suburban sites of New Delhi, India in winter. *Journal of Geophysical Research: Atmospheres*, 127, e2021JD035342. <https://doi.org/10.1029/2021JD035342>

Received 31 MAY 2021

Accepted 17 MAY 2022

Author Contributions:

Conceptualization: Nidhi Tripathi, L. K. Sahu

Data curation: Nidhi Tripathi, Liwei Wang, Pawan Vats, R. V. Satish, Ravi Sahu, Kashyap Patel, Neeraj Rastogi, Dilip Ganguly, Sachchida N. Tripathi

Formal analysis: Nidhi Tripathi, Liwei Wang, Meghna Soni, Kashyap Patel

Investigation: Nidhi Tripathi, Liwei Wang, Pawan Vats, Meghna Soni

Methodology: Nidhi Tripathi, L. K. Sahu, Pawan Vats, Narendra Ojha

Project Administration: L. K. Sahu, André S. H. Prévôt, Sachchida N. Tripathi

Resources: Nidhi Tripathi, Dilip Ganguly

Software: Nidhi Tripathi, Meghna Soni, Kashyap Patel, Narendra Ojha

Supervision: Nidhi Tripathi, Dilip Ganguly

Validation: Nidhi Tripathi, Dilip Ganguly

Visualization: Nidhi Tripathi, Dilip Ganguly

Writing—original draft: Nidhi Tripathi, Dilip Ganguly

Writing—review & editing: Nidhi Tripathi, Dilip Ganguly

Final approval: Nidhi Tripathi, Dilip Ganguly

Project administration: L. K. Sahu, André S. H. Prévôt, Sachchida N. Tripathi

Resources: Nidhi Tripathi, Dilip Ganguly

Software: Nidhi Tripathi, Meghna Soni, Kashyap Patel, Narendra Ojha

Supervision: Nidhi Tripathi, Dilip Ganguly









Validation: Nidhi Tripathi, Dilip Ganguly

Visualization: Nidhi Tripathi, Dilip Ganguly

Writing—original draft: Nidhi Tripathi, Dilip Ganguly

Writing—review & editing: Nidhi Tripathi, Dilip Ganguly

Characteristics of VOC Composition at Urban and Suburban Sites of New Delhi, India in Winter

Nidhi Tripathi^{1,2} , L. K. Sahu¹ , Liwei Wang³, Pawan Vats⁴, Meghna Soni^{1,2}, Purushottam Kumar^{5,6} , R. V. Satish^{1,7} , Deepika Bhattu^{3,8}, Ravi Sahu⁵, Kashyap Patel¹, Pragati Rai³ , Varun Kumar³, Neeraj Rastogi¹ , Narendra Ojha¹ , Shashi Tiwari⁹, Dilip Ganguly⁴, Jay Slowik³, André S. H. Prévôt³, and Sachchida N. Tripathi⁵ 

¹Physical Research Laboratory (PRL), Ahmedabad, India, ²Indian Institute of Technology Gandhinagar Palaj, Gandhinagar, Gujarat, India, ³Laboratory of Atmospheric Chemistry, Paul Scherrer Institute, Villigen, Switzerland, ⁴Centre for Atmospheric Sciences, Indian Institute of Technology Delhi, New Delhi, India, ⁵Department of Civil Engineering and Centre for Environmental Science and Engineering, Indian Institute of Technology Kanpur, Kanpur, India, ⁶Now at Department of Civil and Environmental Engineering, Virginia Tech, Blacksburg, VA, USA, ⁷Now at Department of Environmental Science and Analytical Chemistry, Stockholm University, Stockholm, Sweden, ⁸Now at Department of Civil and Infrastructure Engineering, Indian Institute of Technology Jodhpur, Jodhpur, Rajasthan, India, ⁹Department of Civil Engineering, Manav Rachna International Institute of Research and Studies (MRIIRS), Faridabad, Haryana, India

Abstract Simultaneous measurements of volatile organic compounds (VOCs) using two PTR-TOF-MS instruments were conducted at urban and suburban sites of New Delhi during the winter of 2018. The time series of VOC mixing ratios show substantial variations mainly influenced by local emissions and meteorological conditions. Mixing ratios of methanol (~28 ppbv), acetaldehyde (7.7 ppbv), acetone (10.6 ppbv), isoprene (2.8 ppbv) and monoterpenes (0.84 ppbv) at the suburban site were higher than those at the urban site, while levels of aromatic VOCs were almost similar. The strong nighttime correlations of isoprene and monoterpenes with CO and benzene at the urban site indicate their predominant anthropogenic origin. Higher emission ratios of $\Delta\text{VOCs}/\Delta\text{CO}$ and $\Delta\text{VOCs}/\Delta\text{benzene}$ than those reported for vehicular exhaust suggest the contributions of other sources. In addition to vehicular emissions, episodes of biomass burning, industrial plumes and aged air strongly influenced the levels of VOCs at the suburban site. Despite the predominant primary anthropogenic emissions, the higher daytime enhancements of OVOCs/CO ratios indicate additional contributions of OVOCs from secondary/biogenic sources. The secondary formation of OVOCs in moderately aged air masses was noticeable at the suburban site. Using the source-tracer-ratio method, the estimated biogenic contributions of isoprene (71%) and acetone (65%) during daytime at the suburban site were significantly higher than those for the urban site. The photochemical box model simulations suggest that daytime ozone formation was under the VOC-limited regime. The present study highlights the impact of different emission sources, photochemical processes and meteorological conditions on the composition and concentration of VOCs in the Delhi region.

Plain Language Summary Contributions of natural and anthropogenic sources of volatile organic compounds (VOCs) vary on local and regional scales. In recent years, emission from the use of fossil fuels is the main anthropogenic source of ambient air VOCs in the urban regions of developing countries. Other sources such as biomass/biofuel burning and biogenic emissions also influence urban air quality in tropical regions. The distinction between biogenic and anthropogenic contributions of VOCs in urban air is not straightforward because many VOCs are emitted from several co-located sources. In this study, we performed simultaneous VOC measurements using state-of-art instruments at the urban and suburban sites of New Delhi in the polluted Indo-Gangetic Plains of India during the winter season. Besides the impact of primary sources, we have also investigated the roles of photochemical secondary formation of oxygenated VOCs. Our findings will help policymakers develop strategies for controlling primary and secondary pollutants in this tropical urban region.

1. Introduction

Volatile organic compounds (VOCs) are ubiquitous organic gases present in the Earth's atmosphere at trace levels (pptv-ppbv). Typically, VOCs are categorized into two major groups of non-methane hydrocarbons (NMHCs) and oxygenated-VOCs (OVOCs). NMHCs are primary VOCs emitted from biogenic and anthropogenic sources,

Supervision: L. K. Sahu, André S. H.

Prévôt, Sachchida N. Tripathi

Validation: Nidhi Tripathi, Narendra Ojha

Visualization: L. K. Sahu, Jay Slowik, André S. H. Prévôt

Writing – original draft: Nidhi Tripathi, Purushottam Kumar

Writing – review & editing: L. K. Sahu, Deepika Bhattu, Pragati Rai, Neeraj Rastogi, Narendra Ojha, Shashi Tiwari, Dilip Ganguly, Jay Slowik, André S. H. Prévôt, Sachchida N. Tripathi

whereas both primary and photochemical/secondary sources contribute to OVOCs (C. Liu, Ma, et al., 2017; C. Liu, Zhang, et al., 2017; Sahu, Pal, et al., 2016; Sahu, Yadav, & Pal, 2016). However, based on their major global emission sources, VOCs are also classified as anthropogenic VOCs (AVOCs) and biogenic VOCs (BVOCs). According to the Model of Emissions of Gases and Aerosols from Nature Monitoring Atmospheric Composition and Climate project (MEGAN-MACC) estimates of global BVOC emissions, isoprene (C_5H_8) contributes ~70% to the average total emission (Sindelarova et al., 2014). Monoterpenes (MTs, $C_{10}H_{16}$), methanol (CH_3OH), acetone (CH_3COCH_3), sesquiterpenes, and other BVOC species account for ~11, 6%, 3%, 2.5%, and 2%, respectively. In the troposphere, VOCs are precursors for the formation of secondary organic aerosols (SOA) and ozone (O_3) in the presence of oxides of nitrogen ($NO_x = NO + NO_2$) and sunlight (Hester & Harrison, 1995; Seinfeld & Pandis, 2016). Most of VOCs can rapidly react with hydroxyl radicals (OH), O_3 and nitrate radical (NO_3) and can influence the oxidation capacity of the atmosphere. Therefore, the levels of VOCs in the global atmosphere can change the lifetimes of long-lived compounds such as methane (CH_4) (Lelieveld et al., 2008; Monks, 2005).

Although associated with large uncertainties, the global emissions of $\sim 1,000$ Tg year $^{-1}$ of VOCs estimated from biogenic sources (Guenther et al., 2006, 2012) is ~ 10 times greater than those from anthropogenic sources (Goldstein & Galbally, 2007). However, the balance between biogenic and anthropogenic emissions can vary greatly at local and regional scales. Ambient air measurements of VOCs over several urban and industrial regions of the world revealed the dominant contribution from anthropogenic sources (e.g., de Gouw et al., 2009; Wu & Xie, 2018). The major anthropogenic sources in the urban environment include fossil fuel combustion, biomass/biofuel burning, fuel evaporation, use of solvents, and industrial processes (Duan et al., 2008; Legreid et al., 2007; Sawyer et al., 2000). The contributions of secondary sources via photo-oxidation of primary VOCs are also significant in the urban atmosphere (Friedman et al., 2017; Yuan et al., 2012). Several studies have reported that alcohols (methanol and ethanol), ketones (especially acetone) and aldehydes (formaldehyde and acetaldehyde) are the most abundant OVOCs measured in the urban air (Acton et al., 2020; de Gouw et al., 2018; Wu et al., 2020). Nonetheless, the understanding of different emission and atmospheric processes of VOCs is important to assess their impact on air quality in complex urban environments (Warneke et al., 2013).

Several urban regions of India have been facing prolonged episodes of severe air pollution due to rapid urbanization and ever-increasing numbers of vehicles (Majumdar et al., 2011; Ramachandra, 2009). In India, the major anthropogenic sources of VOCs include emissions from residential combustion (~41%), transportation (37%), and industrial combustion (13%) (Li et al., 2014). The Indo-Gangetic plain (IGP) experiences elevated loadings of gaseous and particulate pollutants from local and regional sources (Dey et al., 2012; Guttikunda et al., 2014; Kaskaoutis et al., 2014; Sen et al., 2017; Srivastava et al., 2014). In the winter season, the ambient pollution is aggravated by stagnant meteorological conditions resulting in smog formation and visibility reduction across the IGP (Ojha et al., 2020). Therefore, it is important to understand the role of emission, photochemistry, and meteorology in governing ambient air pollution over this part of the world. Effective O_3 concentration control strategies are required considering significant impacts on human health and crop yields (Anenberg et al., 2010; Feng et al., 2019; Li et al., 2017; WHO, 2017). The implementation of such strategies needs an adequate understanding of the nonlinear VOC- NO_x - O_3 chemistry. Modeling studies have provided first-hand information about the sensitivity of O_3 formation to the background levels of NO_x and VOCs (e.g., Chen et al., 2021; Goldberg et al., 2016; Ojha et al., 2012; Sillman et al., 2003; Tang et al., 2010; Xue et al., 2013). However, modeling studies in the tropical Indian region are relatively few and reveal strong biases when simulations are compared with observations (Chutia et al., 2019; David et al., 2019; David & Ravishankara, 2019; Kumar et al., 2012; Mahajan et al., 2015; Sharma et al., 2017; Surl et al., 2018). These biases have been suggested to be due to uncertainties in the input emissions and model resolutions, besides the treatment of atmospheric chemistry in different mechanisms. Recent studies have shown substantial improvements in the forecasts through the assimilation of observational datasets in the model (Jena et al., 2021; Kumar et al., 2020). In view of this scenario, in situ measurements in different environments are needed to characterize the sensitivity of O_3 to its precursors and improve the performances of regional and global models. Model-based estimates of emission inventories of various VOCs are reported with significant uncertainties for major urban areas of developing countries (e.g., Karl et al., 2009; Ohara et al., 2007). Real-time speciated measurements of VOCs and reference trace gases (e.g., CO) provide important datasets to estimate urban emission factors (Brito et al., 2015).

The studies characterizing the emission and photochemical processes of VOCs and O_3 in the urban regions of India are limited mainly due to the lack of comprehensive real-time measurements (Sahu, Yadav, & Pal, 2016;

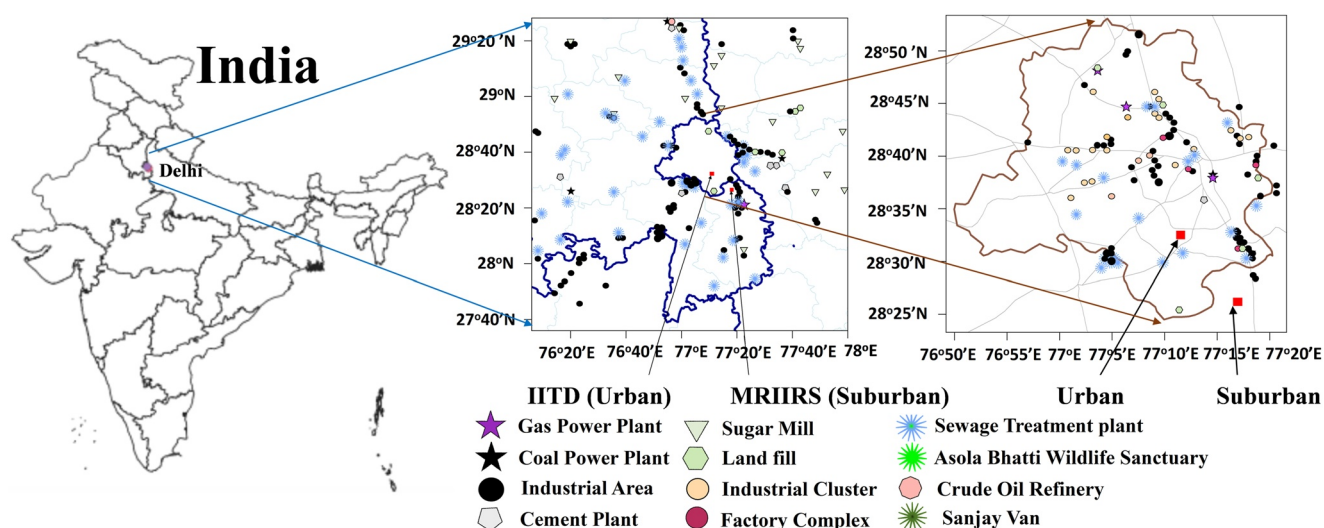


Figure 1. The left panel shows the locations (red square) of IITD urban and MRIIRS suburban sites and industrial estates on the map of New Delhi and surrounding regions. The right panel shows the locations of different industries near the IITD urban site on the map of the National Capital Territory (NCT) of New Delhi.

Sahu et al., 2020; L. Wang et al., 2020). The present study is based on the simultaneous measurements of VOCs using two Proton Transfer Reaction Time-of-Flight Mass Spectrometer (PTR-TOF-MS) instruments at an urban and a suburban site of New Delhi, India during the winter season of 2018. The high time- and mass-resolved measurements of various VOCs were analyzed to assess the impact of different emission sources, episodic events, photochemical processes and meteorological conditions. We have investigated the change in the concentration and composition of VOCs in different air masses with respect to the tracer compounds for primary emissions. The contributions of anthropogenic, biogenic/secondary sources to different VOCs in ambient air were quantified by the source-tracer-ratio method. The photochemical age-based method was applied to investigate the role of secondary formation of OVOCs in ambient air. The photochemical box model simulations were performed to study the O_3 variability due to variations in VOCs and NO_x . The ozone formation potential (OFP) and OH reactivity of different VOCs were estimated to understand their relative importance in the O_3 formation.

2. Materials and Methods

2.1. Site Description

India's capital New Delhi is one of the largest megacities in the world. The city lies in the IGP with the Thar Desert in the west, the central plains in the south, and the Himalaya in the northeast (Gurjar et al., 2016). The major local pollution sources include vehicular traffic, industries, and power plants, besides regional biomass/biofuel burning sources (Rai et al., 2020). The instruments were deployed in the campuses of Indian Institute of Technology Delhi (IITD; 28.54°N, 77.19°E) and Manav Rachna International Institute of Research and Studies (MRIIRS; 28.45°N, 77.28°E) representing urban and suburban areas, respectively. The suburban site (downwind region) is located at a distance of ~20 km in the southeast (SE) direction from the urban site (IITD) (Figure 1). At IITD, the instruments were installed on the third floor of the Centre for Atmospheric Science laboratory building. The IITD site is situated at a distance of ~80 m from a major road known as the outer ring road. In addition to traffic-related emissions, the measurements at IITD were influenced by the emissions from industries located in the surrounding areas (Figure 1 and Figure S1 in Supporting Information S1).

At the MRIIRS site, the instruments were deployed on the first floor of the Civil Engineering building. The MRIIRS campus, located in the Faridabad suburb, is an outskirts area of New Delhi. This site is located at a distance of ~100 m in the west of a national highway (NH-2) connecting two states (provinces) of New Delhi and Haryana and at a distance of ~3 km from the Mathura road (NH-19). The MRIIRS site is surrounded by several vegetated areas (Asola Wild Life Sanctuary), industrial and chemical plants within 1–5 km of distances (Figure 1 and Figure S1b in Supporting Information S1).

The vehicular traffic in New Delhi consists of both light-duty vehicles (LDVs) and heavy-duty vehicles (HDVs). Usually, the emissions from LDVs dominate during the morning (07–10 hr) and evening (18–21 hr) rush-traffic hours. The emissions from HDVs are highest during nighttime (21–07 hr).

2.2. Measurement Techniques

Measurements of VOCs were conducted using PTR-TOF-MS 8000 instruments (Ionicon Analytical G.m.b.H, Innsbruck, Austria) from January 10 to 07 March 2018. The PTR-TOF-MS 8000 provides high time- and mass-resolution measurements of various VOCs. Measurements at both sites were performed using similar operating parameters (e.g., drift tube pressure of 2.3 mbar, drift temperature of 60°C, and drift voltage of 660 V). The ratio of the electric field (E) to gas number density (N) in the drift tube was set between 128 and 130 Townsend (1 Townsend = 10^{-17} V cm²). The E/N ratio in the range of 110–130 Td, where hydration and fragmentation are minimized, has been suggested for the standard ambient air measurements (Hewitt et al., 2003). Very high-purity hydronium ions (H_3O^+) are produced in the ion source region. Subsequently, H_3O^+ ions enter the drift tube where the proton transfer reactions occur between H_3O^+ and any compounds with higher proton affinity (PA) than that of H_2O (691 kJ mol⁻¹). The ambient air samples were drawn into the drift tube through a 1.5 m long heated (60°C) Teflon® PFA tube (1/8" or 3.175 mm) at a flow rate of ~60 mL min⁻¹. A VOC molecule (R) is ionized in the drift tube by the following proton transfer reaction.



The proton transfer reaction rate coefficients vary in the range of $1.5\text{--}3.9 \times 10^{-9}$ cm³ s⁻¹ (Smith & Španěl, 2005) and a typical value of (2×10^{-9} cm³ s⁻¹) has been used here to calculate VOC concentrations. The ionized molecules (RH^+) enter the time of flight (TOF) chamber and get separated according to the mass-to-charge ratio (m/z) and finally detected by the multi-channel plate (MCP) detector. Instead of $H_3^{16}O^+$ (m/z 19.0178) ions, which can saturate the MCP, we used the signal of $H_3^{18}O^+$ (m/z 21.0221) to quantify the concentrations of reagent ions by assuming a natural ratio of $^{16}O/^{18}O$ (~500:1). The spectra measured at time resolution (integration) of 30 s were stored in "hdf5" format using the TOF-Daq program, and quantification of peaks at different masses was performed using the PTR-TOF Data Analyzer (Graus et al., 2010). Under typical operating condition for ambient air measurements, a mass-resolving power ($m/\Delta m$) of about 5,000 (FWHM) was achieved (Sahu, Yadav, & Pal, 2016). A certified standard gas mixture (L5388, Ionicon Analytik GmbH Innsbruck) containing ~1.0 ppmv of 13 different VOCs with protonated mass of (a) OVOCs; m/z 33.034 (methanol), 45.034 (acetaldehyde), 59.049 (acetone), 47.050 (ethanol), and 73.065 (methyl ethyl ketone, MEK), (b) aromatics, m/z 79.054 (benzene), 93.070 (toluene), 107.086 (C_8 aromatics, including ethylbenzene and xylenes), 42.034 (acetonitrile), 69.070 (isoprene), 113.016 (chlorobenzene), 137.133 and 81.07 (MTs and its fragment), and 146.977 (1,2 dichlorobenzene) was used to generate their sensitivity curves (Wang et al., 2020). The different known (set) volume mixing ratios were obtained by dynamic dilutions of the standard mixture using a "gas calibration unit" (GCU-advanced v2.0, Ionicon Analytik) for multipoint calibration. The instrument baseline was determined by analyzing the response of VOC-free zero air generated using VOC scrubber catalyst heated at 350°C in the GCU. The flow rate of the standard mixture was adjusted using a mass flow controller (MFC_{std}) onto the flow (500 sccm min⁻¹) of dilution gas (zero air) maintained using MFC_{dil} to produce variable known mixing ratios. The zero air in GCU was produced by passing ambient air through a heated (350°C) VOC-scrubber catalyst. A stable supply of zero air is important for the determinations of background signals and hence to quantify the overall performance of PTR-TOF-MS including sensitivity. The desired relative humidity (RH) of zero-air air was generated by adjusting the set dew point temperature in the dew point mirror (DPM) in GCU. The instrumental background and calibration at different RH values were performed about every 3- and 10-day of intervals, respectively. Additional details of the operation, calibration procedures and fragmentation of MTs are described in our previous studies (Sahu, Yadav, & Pal, 2016, 2017; Tripathi & Sahu, 2020). The measurement precisions of VOCs presented in this paper varied in the range of 2%–15%. The uncertainties (8%–13%) in the calculations of the mixing ratios of VOCs include the uncertainties in the mass flow controllers (MFCs) of GCU and standard mixture ($\pm 5\%$ –6%) (Sahu & Saxena, 2015; Tripathi & Sahu, 2020).

The fragments of several compounds, such as cyclopentene, pentanal, and 2-methyl-3-buten-2-ol (MBO) can interfere with the isoprene (m/z 69.0699) signal detected using the PTR-TOF-MS (e.g., Sahu, Yadav, & Pal, 2016). The mixing ratios of these interfering compounds are found to be particularly significant near the petrochemical

facilities (Warneke et al., 2010). However, the measurement sites are far away from the petrochemical industrial sources. We have compared the PTR-TOF-MS measurements with TD-GC-FID at similar urban site of Ahmedabad, India. Based on comparison of ambient isoprene measurements, the $(\text{PTR-TOF-MS})_{\text{isoprene}}/(\text{TD-GC-FID})_{\text{isoprene}}$ ratio of ~ 1.04 was determined which indicates a good agreement between the two instruments. The strong correlation between m/z 137.133 and m/z of 81.07 indicates that the interferences of other sources to MTs were negligible (Figure S2 in Supporting Information S1). Therefore, the impact of possible interference from other compounds to isoprene and monoterpenes is assumed to be negligible.

The mixing ratios of O_3 , carbon monoxide (CO), and NO_x measured during the campaign were used as supporting data. At MRIIRS, the 49i, 48i, and 42i analyzers (Thermo Scientific, US) were used for the online measurements of O_3 , CO, and NO_x mixing ratios, respectively. At IITD, Serinus 30 and Serinus 40 Ecotech analyzers were operated for the measurements of CO and NO_x mixing ratios, respectively.

2.3. Model Description

The dependence of O_3 variability on precursors at the suburban and urban sites was analyzed by conducting simulations using the Master Mechanism v2.5 model (Chen et al., 2021). The model includes detailed gas-phase chemistry of about $\sim 2,000$ different chemical species (Madronich, 2006). Photolysis rates are calculated using the Tropospheric Ultraviolet and Visible (TUV) radiative transfer model (version 5.0), which is coupled with the Master Mechanism box model (Madronich & Flocke, 1999). Further details of this model and its applications over the Indian region can be found elsewhere (Chen et al., 2021; Madronich, 2006; Ojha et al., 2012).

The environmental conditions chosen in the simulations for the suburban and urban sites are summarized in Table S1 in Supporting Information S1. The values of total O_3 column and single scattering albedo are obtained from the OMI satellite data and Modern-Era Retrospective analysis for Research and Applications, Version 2 (MERRA-2) model reanalysis, respectively. While aerosol optical depth at 550 nm and Angstrom coefficient are taken from MODIS-Aqua satellite data. The model is initialized using the average values of CO, NO_x , and various VOCs derived from observations during the present campaign. The mixing ratios of methane (2.25 ppmv) and key light NMHCs including ethane (20 ppbv), ethene (14 ppbv), propane (29 ppbv), propene (4 ppbv), i-butane (11 ppbv), n-butane (22 ppbv), acetylene (10 ppbv), i-pentane (8 ppbv), n-pentane (6 ppbv), and 1-pentene (0.1 ppbv) have been included for model inputs. NMHCs were measured using a $\text{C}_2\text{--C}_6$ VOCs analyzer (AirmoVOC, Model: A22022, Chromatotec®, France) at the IITD site during the winter season of 2019. Methane was set to 2.25 ppm by considering the observed urban and industrial influences in Delhi's environment (Sahay & Ghosh, 2013).

2.4. Determination of VOC Emission Ratios

At the time of emission, each VOC has a characteristic molar emission ratio (ER) depending on the source type. The ER of a compound (X) with respect to a reference or tracer compound (Y) can be given as:

$$\text{ER} = \frac{\Delta X}{\Delta Y} = \text{Slope of the } X \text{ with } Y \quad (2)$$

Several studies have used the ER of VOCs to CO to characterize their emissions from a particular source (e.g., Borbon et al., 2013; Yuan et al., 2012). The ambient air molar mixing ratio of CO has been used as a tracer for incomplete combustion-related emissions (Chandra et al., 2016). The measured molar ratio (X/Y) at any given time has been used to estimate the ER by applying the corrections due to the photochemical process known as age-corrected ER (e.g., Baker et al., 2011; de Gouw et al., 2001; Thorenz et al., 2017). The measurements from midnight to early morning hours are strongly impacted by direct emissions and used to determine the ERs of VOCs (Borbon et al., 2013; Parrish et al., 2012; Warneke et al., 2007). We refer the readers to Akagi et al. (2011) for a more detailed description of ER parameters. In this study, we have calculated the ERs of several VOCs to identify the emissions sources and estimate the photochemical age.

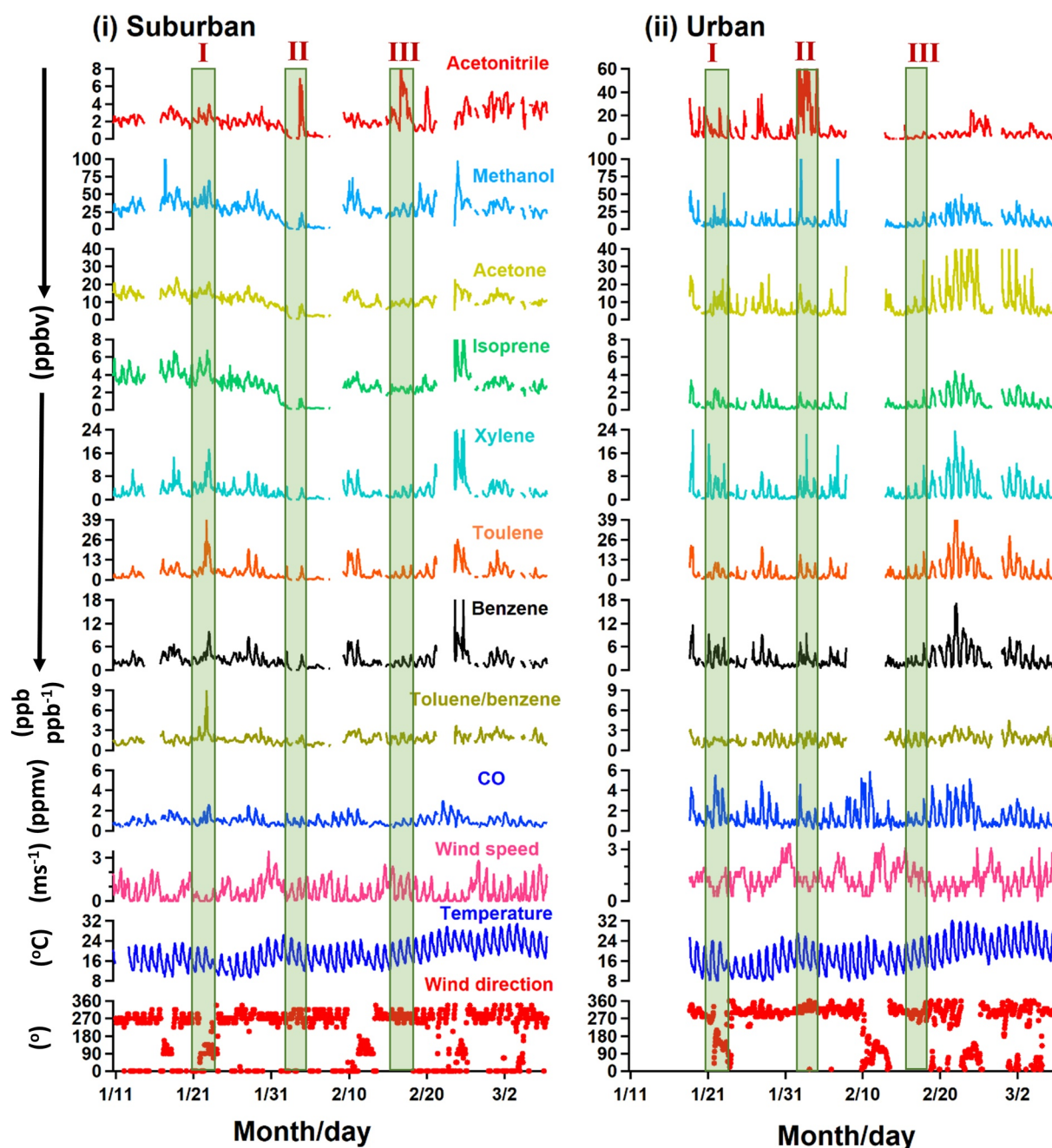


Figure 2. Time series of VOCs, CO, wind speed, temperature and wind direction at (i) MRIIRS suburban (left panel) and (ii) IITD urban (right panel) sites in New Delhi, India from 10 January to 8 March 2018. The three semi-transparent strips (I, II, III) represent the different episodic events observed during the measurement period.

3. Results and Discussion

3.1. The Characteristics of VOC Levels and the Impact of Meteorological Conditions

The hourly time series of VOCs, CO, NO_x , temperature and wind speed measured at both sites are plotted in Figures 2 and 3. The variations of the planetary boundary layer height (PBLH) using the ERA5 data (the fifth generation ECMWF atmospheric reanalysis) are shown in Figure 3 (Hersbach et al., 2018). Although a few studies have suggested overall consistency between the ECMWF reanalysis, WRF model and observations over northern India (e.g., Brunamonti et al., 2019), there can be some significant biases between the model and local

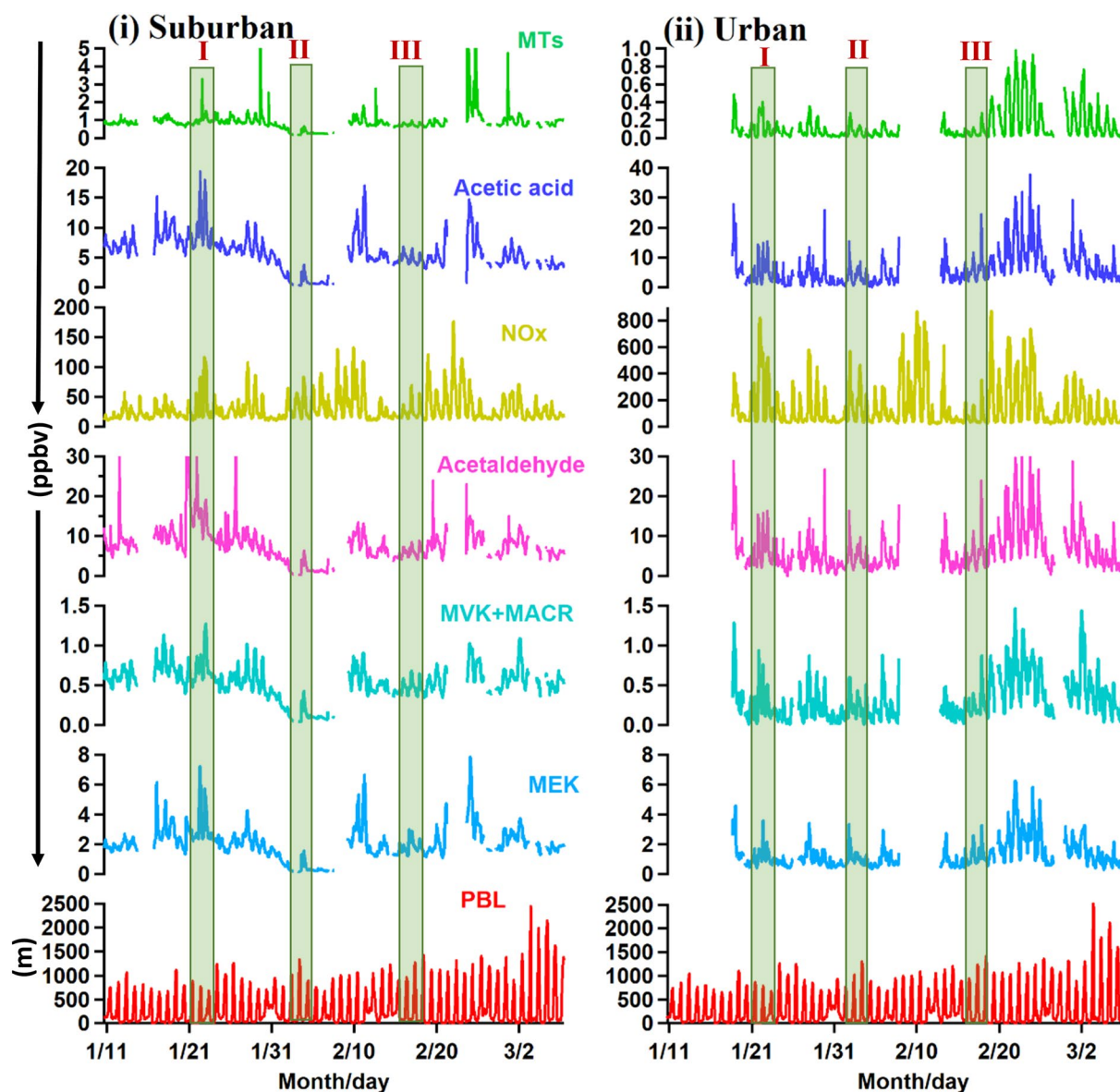


Figure 3. The time series plots of VOCs, NO_x , and the planetary boundary layer (PBL) depth at (i) MRIIRS suburban (left panel) and (ii) IITD urban (right panel) sites in New Delhi. The PBL data are taken from ERA5 (the fifth generation ECMWF atmospheric reanalysis) (Hersbach et al., 2018).

observations of PBLH (Nakoudi et al., 2019). In this study, we have used PBLH data to investigate the effect of the boundary layer dynamics in ambient air variations of VOCs.

VOCs as well as other trace gases show large variations at both sites. At the urban site, the daily average mixing ratios of isoprene, MTs, methanol, benzene and toluene were in the ranges of 0.2–2.4, 0.03–0.6, 3.8–34.3, 1.1–7.4, and 1.1–19.9 ppbv, while at the suburban site these were in the ranges of 0.16–5.70, 0.24–2.39, 2.52–47.23, 0.73–6.03, and 0.69–16.39 ppbv, respectively. The levels of BVOCs and OVOCs at the suburban site were higher than those measured at the urban site. The average mixing ratios of isoprene and monoterpene at the suburban site are ~ 3 and 6 times higher than their levels at the urban site, respectively. Nevertheless, the levels of aromatic compounds such as toluene (~ 5 ppbv), benzene (3 ppbv), and xylene (3 ppbv) are similar for both urban and suburban sites. The mixing ratios of CO (0.63–2.88 ppmv) and NO_x (30.4–507 ppbv) at the urban site were higher than their values (CO = 0.51–1.67 ppmv and NO_x = 12–65 ppbv) measured at the suburban site. However, particularly during the northwest (NW) winds, the suburban site is downwind of major city centers including the urban site (Figure S3 in Supporting Information S1). The transport time of air masses from the upwind urban

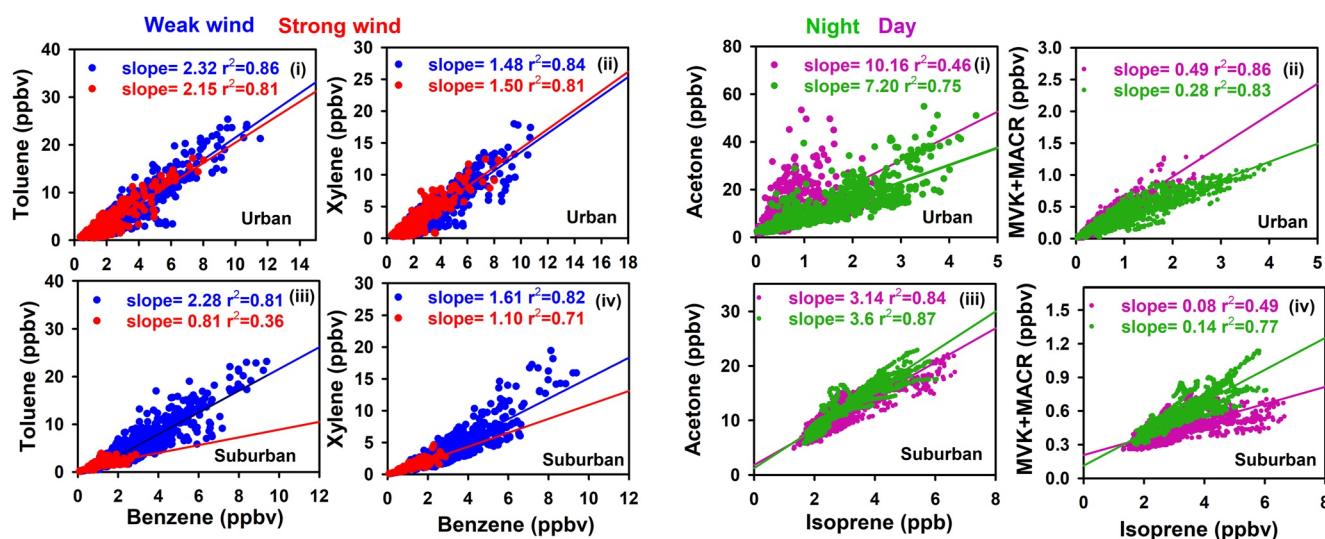


Figure 4. (a) Scatter plots of the mixing ratios of toluene and xylene with benzene for the urban [(i) and (ii)] and suburban [(iii) and (iv)] sites under the calm ($\leq 1.2 \text{ m s}^{-1}$) and stronger ($> 1.2 \text{ m s}^{-1}$) wind conditions. (b) Scatter plots of the mixing ratios of acetone and MVK + MACR with isoprene for the urban [(i) and (ii)] and suburban [(iii) and (iv)] sites of New Delhi during the day and night hours.

region to downwind suburban areas is about 1 hour as estimated using the Hybrid Single-Particle Lagrangian Integrated Trajectory (HYSPLIT) model simulation. Therefore, the time series at both sites show similar trends except when the southeast (SE) winds prevailed. However, as discussed in the following section, the time series of VOC mixing ratios show some similar and distinct features between the two sites.

The meteorological variations can have significant impacts on the levels of VOCs at both sites. The higher levels of VOCs, except for acetonitrile, were measured during 19–23 February at the urban site and during 20–25 February at the suburban site. Episodically, higher levels of VOCs, CO, and NO_x were observed at the suburban site when winds were from the SE sector housing several industrial units (Figure 1 and Figure S4 in Supporting Information S1). Lower mixing ratios of primary VOCs (e.g., toluene, benzene, and xylene) associated with relatively higher wind speeds ($> 1.2 \text{ m s}^{-1}$) indicated the impact of dilution due to mixing with photochemically aged background air masses. For example, Figure S4d in Supporting Information S1 shows the dependence of the toluene mixing ratio with the wind speed at the suburban site during the entire study period.

The correlations between primary VOCs (toluene, benzene, and xylene) under the calm ($\leq 1.2 \text{ m s}^{-1}$) and stronger ($> 1.2 \text{ m s}^{-1}$) wind conditions are shown in Figure 4a. The criterion for choosing strong and weak winds is discussed in our earlier studies (e.g., Sahu, Yadav, & Pal, 2016). The mixing ratios of benzene and toluene measured under calm/weak winds show stronger correlations ($r^2 > 0.80$) than those under the strong winds (Figure 4a). At the urban site, the slopes of $\Delta\text{Toluene}/\Delta\text{benzene}$ ($\Delta\text{T}/\Delta\text{B}$) and $\Delta\text{xylene}/\Delta\text{benzene}$ ($\Delta\text{X}/\Delta\text{B}$) were ~ 2.32 and $1.48 \text{ ppb ppb}^{-1}$ for calm conditions, and similar values of 2.15 and $1.50 \text{ ppb ppb}^{-1}$ were determined for stronger winds, respectively. The almost similar $\Delta\text{T}/\Delta\text{B}$ and $\Delta\text{X}/\Delta\text{B}$ values under weaker and stronger wind speed regimes at the urban site indicate major emissions of aromatic VOCs from the local sources and lesser impacts of the transport from the distant sources (Sahu et al., 2022). At the suburban site, the $\Delta\text{T}/\Delta\text{B}$ and $\Delta\text{X}/\Delta\text{B}$ slopes of 2.3 and $1.61 \text{ ppb ppb}^{-1}$ determined for the calm conditions were significantly higher than their respective values of 0.81 and 1.1 ppb ppb^{-1} during periods with under the strong winds. In general, calm winds are northerly; strong winds are westerly, where there are no significant anthropogenic sources. It can be noticed that the industrial units of PVC, iron and steel, paper, machinery, gas power, sewage plants, and so forth, are situated north of the suburban site (Figure 1). Several studies have reported that BTEX and acetaldehyde are emitted in significant amounts from PVC, paper mills, coal power plants, landfill, and cement industries (Dave et al., 2020; Evans, 2009; Garcia et al., 1992; Liu et al., 2019; Scott et al., 2020; Tong et al., 2015). In addition, the emission from sewage treatment plants can also be a source of toluene, benzene, xylene, acetone, acetaldehyde and methanol (Byliński et al., 2019; Quigley & Corsi, 1995; Yang et al., 2012). Therefore, the higher levels of aromatic VOCs at the suburban site under calm conditions suggest the influences of the local sources, including industrial emissions. Whereas, lower $\Delta\text{T}/\Delta\text{B}$ and $\Delta\text{X}/\Delta\text{B}$ values measured under the stronger winds result from the

Table 1

The Average Mixing Ratios of VOCs (Standard Deviation) at IITD Urban and MRIIRS Suburban Sites in New Delhi and the Measurements Reported for Different Urban Sites of the World

VOCs (ppbv)	IITD ^a	MRIIRS ^a	Delhi ^b airport	Ahmedabad ^c	Paris ^d	Zurich ^e	Changdao ^f	Beijing ^g	Mohali ^h
Methanol	12.03 (14.17)	28.35 (12.79)	30	17.85	2.35	1.21	5.67 (4.80)	24.32 (20.83)	37.5 (17.9)
Acetaldehyde	6.13 (4.94)	7.65 (7.65)	21	4.99	1.87	0.82	0.63 (0.44)	4.92 (3.66)	6.7 (3.7)
Acetone	8.97 (10.31)	10.63 (4.57)	32	5.35	1.05	1.17	1.85 (0.92)	2.80 (2)	5.9 (3.7)
Isoprene	0.80 (0.76)	2.81 (1.50)	3.8	1.11	0.17	0.06	0.01 (0.01)	1.21 (1.03)	1.9 (0.9)
Benzene	2.82 (2.30)	2.45 (1.64)	4.5	1.98	0.33	0.75	0.55 (0.36)	2.00 (1.74)	1.7 (1.5)
Toluene	5.14 (6.26)	4.46 (4.3)	6.1	4.29	0.54	1.25	0.57 (0.51)	1.94 (1.87)	2.7 (2.9)
Xylene	3.14 (3.58)	3.05 (3.05)	3.2		0.67	0.25			2 (2.2)
MTs	0.14 (0.18)	0.84 (0.57)	1				0.07 (0.06)		
MEK	1.30 (0.92)	1.42 (1.00)	4.7			0.22	0.35 (0.22)		
MVK + MACR	0.32 (0.26)	0.49 (0.87)	2.1		0.09	0.03			
Acetonitrile	7.55 (16.85)	2.26 (1.14)	1.9	0.76	0.55		0.21 (0.12)	0.51 (0.51)	1.4 (0.9)

^aThis study. ^bHakim et al., 2019. ^cSahu et al., 2017. ^dDolgorouky et al., 2012. ^eLegreid et al., 2007. ^fYuan et al., 2013. ^gActon et al., 2020. ^hSinha et al., 2014.

mixing of local emissions with photochemically aged background air masses and fresh air transported from the less-industrialized/polluted western region. In addition to wind parameters, the variations of BVOCs and OVOCs show a clear dependence on the ambient temperature as discussed in Section 3.3. In Section 3.4, we discuss the differences in VOC levels and their interrelationships between day and night (Figure 4b) and the direct and indirect roles of meteorological processes.

In Table 1, the average mixing ratios of VOCs measured in this study are compared with values reported for several other major cities of the world. Methanol levels at the suburban site are significantly higher than the values reported over the European sites (Table 1). Previous studies have reported that emission from heavy-duty diesel-fueled trucks are one of the major sources of OVOCs in the urban areas (e.g., de Gouw et al., 2005; Dolgorouky et al., 2012; Legreid et al., 2007), besides the solvent in coatings and adhesives, disinfectants/indoor air, and so forth (Karl et al., 2018; Li et al., 2019). Biogenic source of OVOCs include emissions from plants and trees present in the urban and surrounding regions (Karl et al., 2018; Sahu, Yadav, & Pal, 2016). Unlike urban regions of the developed nations, the biomass burning in surrounding region of Delhi could also enhance the background concentrations of OVOCs and in particular of methanol. Sinha et al. (2014) have also reported higher methanol levels (~100 ppbv) at Mohali, located at a distance of 250 km in the north of Delhi, mainly due to influences of biomass burning. In conjunction with the study at Mohali, our observations at New Delhi highlight the significance of open biomass burning in affecting the regional distribution of VOCs. The mean mixing ratio of methanol at the suburban site is comparable to the values reported for Beijing, China during the winter season (Acton et al., 2020). The higher mixing ratios of methanol in Beijing, China were attributed to emissions from industrial activities. In Sections 3.2 and 3.5, we examine the reasons for the higher levels of methanol at the suburban site. The concentrations of aromatic VOCs at both sites of New Delhi are found to be considerably lower than their values reported over Beijing, China (Acton et al., 2020; Gu et al., 2019), but are higher than those over Paris, France (Dolgorouky et al., 2012) and Zurich, Switzerland (Legreid et al., 2007). Higher levels of aromatics in New Delhi compared to a major urban region in western India (Ahmedabad) could be due to higher emissions and favorable meteorological conditions. In January, the average temperatures at Ahmedabad and Delhi were 25 and 16°C, respectively (Sahu, Yadav, & Pal, 2016). In winter conditions, the pollutants emitted from various sources get trapped in the lower PBL heights.

3.2. Episodic Events

At the suburban site, the three important episodic events observed during 22 January, 3–4 February, and 16–17 February are highlighted in Figure 2. Another local event on 2 March 2018 was related to the *Holi* bonfire festival. At the suburban site on 22 January (first event), the average mixing ratios of toluene (16.4 ppbv) and xylene (~8 ppbv) were higher than their non-episodic mean values of ~5 and 3 ppbv, respectively. The T/B ratios

increased up to ~ 8 ppb ppb⁻¹ during this period. Typically, the T/B ratios of 2–4 ppb ppb⁻¹ indicate the influence of vehicular emission, while higher values (>4 ppb ppb⁻¹) indicate industrial emissions (Rogers et al., 2006; Velasco et al., 2007).

In the second episode, the mixing ratios of acetonitrile, a biomass burning tracer (e.g., Holzinger et al., 1999), were observed to be enhanced (~ 6 ppbv) from 3 February 15 hr to 4 February 7 hr at the suburban site (Figure 2 and Figure S5a in Supporting Information S1). However, Bruns et al. (2017) and Coggon et al. (2016) have suggested that acetonitrile may not be a suitable tracer for domestic burning in urban areas, instead, furfural can be used as a wood-burning tracer. Fleming et al. (2018) and Pandey et al. (2014) have discussed the emissions of a wide range of VOCs from different biofuel burning/combustion processes such as dung-*angithi* and brushwood-*chulha* in rural parts of India. Huangfu et al. (2021) have reported higher acetonitrile/CO ratios ($1.1\text{--}7.98$ ppb ppm⁻¹) for outdoor biomass burning sources such as wildfire and crop residue burning. In the present study, a strong acetonitrile-CO correlation ($r^2 = 0.90$) and a higher ER of $\Delta\text{acetonitrile}/\Delta\text{CO}$ (~ 8 ppb ppm⁻¹) confirm the impact of biomass burning (Figure S5b in Supporting Information S1). However, just before this episode, the mixing ratios of all VOCs were significantly lower than the non-episodic days at the suburban site. The average mixing ratios of methanol, acetone, benzene, toluene, and xylene were 8, 4, 1.2, 1.4, and 1.1 ppbv, respectively. In addition to the efficient ventilation due to higher wind speed and PBLH, the transport of regionally aged air masses from regions with less anthropogenic activities could be a factor leading to very low levels of VOCs (Figure S5c in Supporting Information S1).

Elevated levels of acetonitrile (>10 ppbv) were observed in the third event during 16–17 February at the suburban site. The poor correlations of acetonitrile with CO, furan and furfural but strong correlations of acetonitrile with formaldehyde indicate the contributions from non-combustion sources (pharmaceutical/industrial) at the suburban site (Coggon et al., 2016) (Figure S6a in Supporting Information S1). The compositions of VOCs during the second and third events were very different from those measured during the *Holi* bonfire festival on 2 March 2018 (Figure S6b in Supporting Information S1). The simultaneous enhancements in the levels of furfural, acetonitrile, CO, methanol, and formaldehyde on 2 March 2018 at the suburban site indicate the effect of wood-burning during the *Holi* festival. The mixing ratios of VOCs and CO show strong correlations with furfural during the *Holi* (Figure S6c in Supporting Information S1). As shown in Figure S6c in Supporting Information S1, the emission ratio $\Delta\text{acetonitrile}/\Delta\text{CO}$ (~ 1.8 ppb ppm⁻¹) is well within the range of values reported for the open biomass burning sources (Bruns et al., 2016; Huangfu et al., 2021).

3.3. Diurnal Variation of VOCs

In addition to day-to-day variability, the large periodic variations on short time-scales (<1 day) of VOCs, CO, NO, and meteorological parameters indicate their strong diurnal dependence at both sites (Figures 5 and 6).

The mixing ratios of all VOCs at the urban site showed a pronounced peak during the evening-midnight period (18–24 hr). The evening peak amplitudes were higher than the morning rush hour period (07–09 hr) values. In the daytime (8–18 hr), the declines of secondary VOCs (except (methyl vinyl ketone + methacrolein (MVK + MACR))) were smaller than those noticed in the mixing ratios of aromatics, CO, and NO. In the afternoon hours, the lower concentrations of VOCs indicate the combined effect of photochemical loss, efficient ventilation due to the deeper boundary layer and reduced vehicular traffic. The higher concentrations from evening to early morning hours were associated with the rush-hour emissions and their accumulation in the shallower nocturnal boundary layer (NBL). The role of photochemical production and biogenic emissions in controlling the daytime levels of OVOCs and BVOCs are discussed in the following sections. The levels of OVOCs (except acetic acid) and BVOCs at the suburban site were higher than their values at the urban site. The mixing ratios of aromatics and CO were approximately similar for both sites during daytime and early morning, but higher levels were observed at the urban site during the nighttime. The variation in the mixing ratio of NO was similar at both sites during the afternoon, but the mean NO level was ~ 20 times higher at the urban site than that at the suburban site during the nighttime (Figure 6).

VOCs/benzene ratios can account for the effects of diurnal changes in anthropogenic emission, meteorology, and PBL heights to an extent (e.g., Filella & Penuelas, 2006; Sahu, Yadav, & Pal, 2016; Tripathi & Sahu, 2020). The average diurnal profiles of ambient air temperature and VOCs/benzene ratios for both the sites are plotted in Figures 6 and 7, respectively. OVOCs/benzene and isoprene/benzene ratios at both sites show strong diurnal

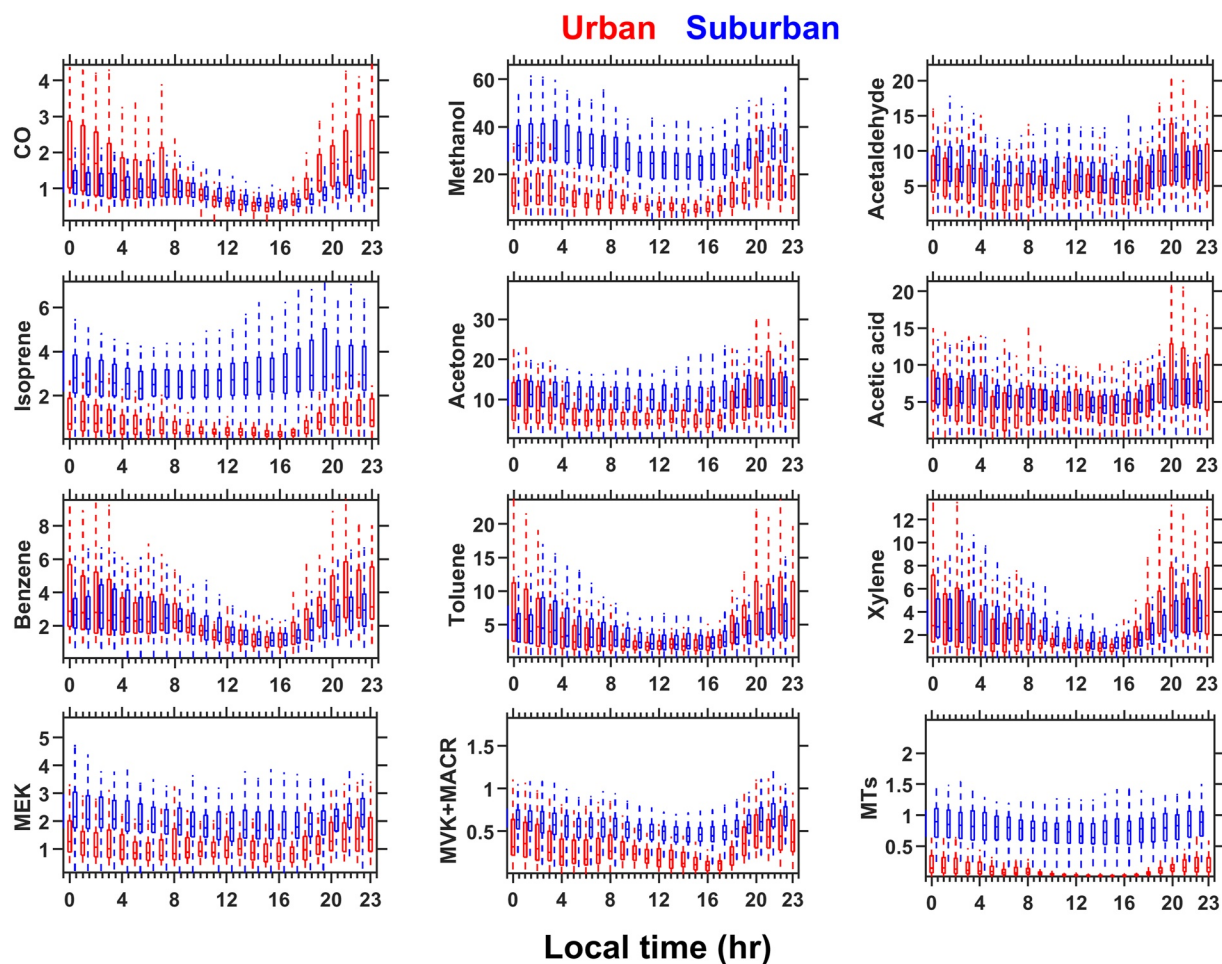


Figure 5. The box-whisker plots showing the diurnal variation of VOCs (ppbv) and CO (ppmv) mixing ratios at the urban and suburban sites in New Delhi during the measurement period.

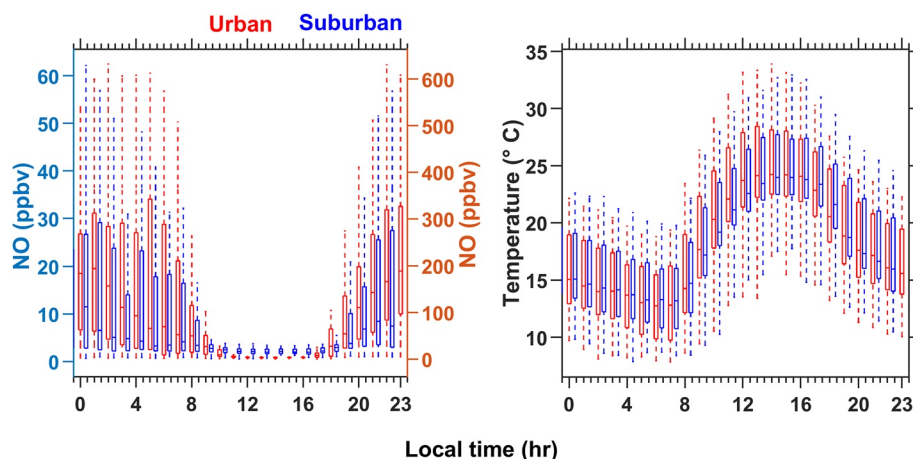


Figure 6. The box-whisker plots showing the diurnal variation of NO mixing ratio and ambient air temperature measured at the urban and suburban sites in New Delhi during the measurement period.

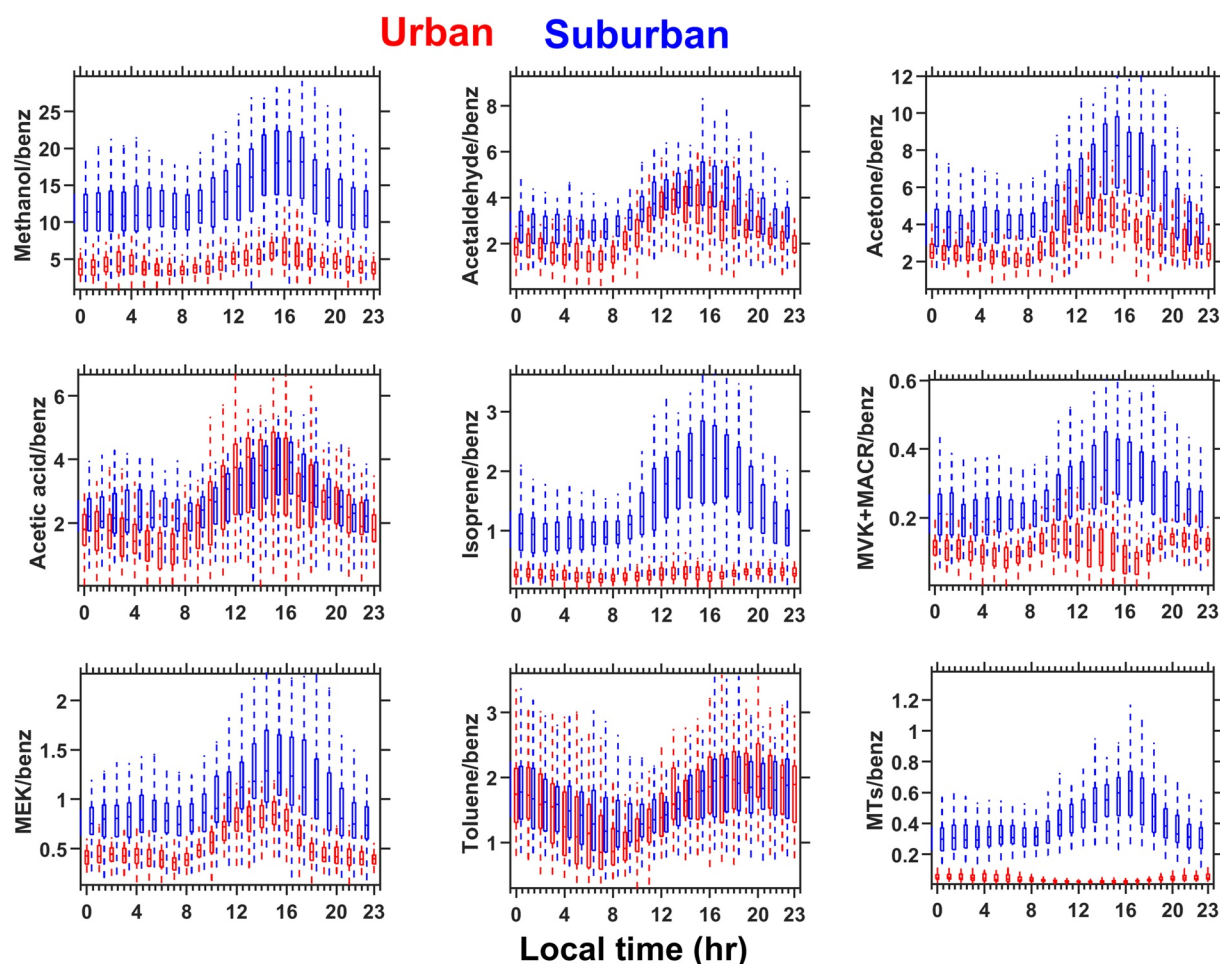


Figure 7. The box-whisker plots showing the diurnal variation of VOCs/benzene ratios (ppb ppb^{-1}) at the urban and suburban sites in New Delhi during the measurement period. In the denominator “benz” stand for benzene.

dependence throughout the study period. The ratio of isoprene/benzene at the urban site increased from $\sim 0.20 \text{ ppb ppb}^{-1}$ at 8 hr to $0.28 \text{ ppb ppb}^{-1}$ at 15 hr. At the urban site, the lower MTs/benzene and MVK + MACR/benzene ratios during the afternoon indicate photochemical loss of MTs and MVK + MACR. The peak values of OVOCs/benzene and isoprene/benzene ratios were observed between 11 and 18 hr at both sites. The higher daytime ratios of OVOCs/benzene could be due to both biogenic and secondary sources at the suburban site. However, the lower daytime ratios of MT/benzene and isoprene/benzene at the urban site indicate negligible biogenic contributions. Therefore, the higher levels of OVOCs/benzene ratios during the daytime were mainly due to secondary formation. In the nighttime, the significant differences of OVOCs/benzene ratios between urban and suburban sites can be attributed to emissions from different anthropogenic sources.

Isoprene is released mainly by chloroplasts and varies as a function of light and temperature (Steeghs et al., 2004). The two main oxidation products of isoprene are MVK + MACR. In the daytime, the enhancements of both isoprene/benzene and MVK + MACR/benzene ratios indicate the impact of biogenic emissions and photo-oxidation in the presence of solar radiation and higher temperatures. However, the isoprene/benzene ratios at the suburban site were ~ 5 times higher than those at the urban site suggesting higher biogenic contributions at the suburban site.

At the suburban site, OVOCs/benzene ratios were low from the night till morning (00–07 hr) but increased from morning till evening (08–18 hr). However, with some lags, the diurnal patterns of OVOCs/benzene tend to follow the temperature cycle. At the suburban site, peaks of VOCs/benzene ratios at around 17 hr could be due to the combined contribution from anthropogenic, biogenic, and secondary sources. At night, the emissions from HDVs

Table 2

The Emission Ratios (ERs) of $\Delta\text{VOCs}/\Delta\text{CO}$ (ppb ppm⁻¹) and $\Delta\text{VOCs}/\Delta\text{Benzene}$ (ppb ppb⁻¹) at IITD Urban and MRIIRS Suburban Sites Estimated Using the Data Measured During 0–5 hr and Comparison of ERs of $\Delta\text{VOCs}/\Delta\text{CO}$ Reported for Different Urban Sites of the World

VOCs	This study $\Delta\text{VOCs}/\Delta\text{CO}$		This study $\Delta\text{VOCs}/\Delta\text{Benzene}$		Different urban cities of the world $\Delta\text{VOCs}/\Delta\text{CO}$					
	IITD	MRIIRS	IITD	MRIIRS	Beijing ^a	Los Angeles ^b	London ^c	Sao Paulo ^d	Beijing ^e	Changdao ^f
Methanol	6.1	20.24	2.36	5.48	10.45	21.72	12	5.39	7.91	16
Acetaldehyde	3.58	5.07	1.47	1.38	2.87	5.42	4.14	3.93	0.86	1.2
Acetone	5.55	5.35	2.05	1.65	1.5	11.78	3.18	3.59	0.93	1.57
Acetic acid	3.63	4.41	1.48	1.35						1.27
MVK + MACR	0.21	0.29	0.06	0.08		0.24				
MEK	0.88	1.14	0.34	0.34	0.55			1.42	0.68	0.47
Isoprene	0.77	1.32	0.31	0.41	0.21	0.3	1.13	1.17	0.06	0.02
Benzene	2.26	3.52	1.00	1.00	1	1.3	1.59	1.03	1.06	1.45
Toluene	5.23	9.16	2.28	2.51	1.33	3.18	3.09	3.1	1.2	2.05
Acetonitrile	1.5	0.63	0.8	0.14	0.39		0.52			0.5
o-xylene	3.35	5.31	1.37	1.58		0.67				
MTs	0.18	0.42	0.07	0.12						
Propanol	0.25	0.18	0.09	0.05		1.13				

^aSheng et al., 2018. ^bBorbon et al., 2013. ^cValach et al., 2014. ^dBrito et al., 2015. ^eWang et al., 2013. ^fYuan et al., 2013.

lead to elevated levels of CO, NO, and aromatic VOCs (Figures 5 and 6). The highest mixing ratios of CO and NO measured at the urban site were ~ 1.6 and ~ 7 times greater than those at the suburban site, respectively. The mixing ratios of aromatic VOCs, CO, and NO_x start increasing at 17 hr due to evening rush-hour traffic. During the same study period, Wang et al. (2020) reported the results of the positive matrix factorization (PMF) analysis of VOCs, showing a traffic-related contribution of 57% at the urban site and 36% at the suburban site.

3.4. Emission Ratios of VOCs

The ERs are determined using the data measured in the midnight to early morning period (00–05 hr) by the linear regression fit (LRF) method (Bon et al., 2011; Borbon et al., 2013). It characterizes emissions primarily from the vehicular exhaust. During the winter season, from midnight to early morning, the contributions from biogenic sources and photochemical processes can be considered negligible in the absence of sunlight (Langford et al., 2010; Tripathi et al., 2021). The mixing ratios of CO and benzene can be used as references for anthropogenic (fossil fuel combustion and biomass burning) and vehicular emissions, respectively (Stockwell et al., 2015). Wagner and Kuttler (2014) have used the ERs of $\Delta\text{VOCs}/\Delta\text{benzene}$ to characterize the vehicular emissions in Essen, Germany. The correlation plots of different VOCs versus CO measured during 00–05 hr are shown in Figure S7 in Supporting Information S1. Most VOCs, including those usually associated with biogenic/photochemical sources, show good correlations with CO. The ERs of $\Delta\text{VOCs}/\Delta\text{CO}$ and $\Delta\text{VOCs}/\Delta\text{benzene}$ estimated for both sites are presented in Table 2 and their correlation coefficient (r^2) values are listed in Table S2 in Supporting Information S1. The ERs of MVK and acetone to isoprene calculated using the daytime (8–18 hr) data are used to characterize the biogenic source and secondary formation.

3.5. Emission Ratios of Primary VOCs

Henze et al. (2008) have described the use of ERs of aromatic VOCs to CO to predict SOA formation in photochemical models. At both sites, benzene and toluene mixing ratios show strong correlations ($r^2 > 0.75$) with CO. The ERs of $\Delta\text{benzene}/\Delta\text{CO}$ (2.26 ppb ppm⁻¹), $\Delta\text{toluene}/\Delta\text{CO}$ (5.23 ppb ppm⁻¹), $\Delta\text{o-xylene}/\Delta\text{CO}$ (3.35 ppb ppm⁻¹), and $\Delta\text{isoprene}/\Delta\text{CO}$ (0.77 ppb ppm⁻¹) estimated for the suburban site are ~ 1.5 times greater than those for the urban site. The ERs of aromatic VOCs to CO determined for both sites are higher than those reported for other megacities of the world (Table 2). In the Los Angeles (LA) basin, USA (Warneke et al., 2013), the ERs of $\Delta\text{benzene}/\Delta\text{CO}$ and $\Delta\text{toluene}/\Delta\text{CO}$ were 1.27 and 3.11 ppb ppb⁻¹, respectively. Although vehicle exhaust is a

major source in New Delhi, the higher ERs of aromatic VOCs than those for other megacities indicate the higher contributions from non-traffic local sources such as the use of solvent, evaporation loss and industrial emissions. Therefore, the differences in the nighttime ERs of $\Delta\text{VOCs}/\Delta\text{CO}$ between New Delhi and other megacities could result from different fuel compositions and varying contributions from other sources. However, to some extent, the differences in measurement methods could be another factor leading to the differences in the values of ERs reported for the different cities.

The strong correlations ($r^2 > 0.7$) of isoprene with CO and benzene during the nighttime at the urban site indicate the dominant emission of isoprene from vehicles. At the suburban site, isoprene showed a weak correlation ($r^2 = 0.36$) with CO and a moderate correlation ($r^2 = 0.54$) with benzene. Almost all VOCs showed strong correlations with benzene, indicating their emissions mainly from vehicles followed by contributions from other combustion-related sources. The ERs of $\Delta\text{isoprene}/\Delta\text{CO}$ ($0.77\text{--}1.32\text{ ppb ppm}^{-1}$) estimated in this study are comparable to the values for Sao Paulo and London. Sahu et al. (2017) have reported significant anthropogenic contributions to ambient concentrations of isoprene at a major urban site of Ahmedabad in western India during the winter season. The ERs of $\Delta\text{isoprene}/\Delta\text{benzene}$ at urban (0.31 ppb ppb^{-1}) and suburban (0.41 ppb ppb^{-1}) sites show a reasonable agreement with those for Los Angeles (0.30 ppb ppb^{-1}) and London (0.71 ppb ppb^{-1}) indicating significant emissions from vehicular sources in New Delhi.

3.6. Emission Ratios of OVOCs

The mixing ratios of OVOCs showed moderate to good correlations ($r^2 = 0.5\text{--}0.8$) with CO at both sites. Methanol shows a stronger correlation with CO ($r^2 = 0.77$) at the suburban site than at the urban site. The ERs of $\Delta\text{methanol}/\Delta\text{CO}$ (20.2 ppb ppm^{-1}), $\Delta\text{acetone}/\Delta\text{CO}$ (5.4 ppb ppm^{-1}), and $\Delta\text{acetaldehyde}/\Delta\text{CO}$ (5.1 ppb ppm^{-1}) estimated for the suburban site are greater than those for the urban site. As presented in Table 2, the ER of $\Delta\text{methanol}/\Delta\text{CO}$ (6.1 ppb ppm^{-1}) estimated for urban site is within the range of values reported for other megacities of the world. At the suburban site, the ER of $\Delta\text{methanol}/\Delta\text{CO}$ is comparable to the values reported for Sao Paulo and Beijing but higher than that for other cities except for Los Angeles. The ERs of $\Delta\text{OVOCs}/\Delta\text{CO}$ were lowest for Mexico City (methanol = 2.1, acetone = 0.51, acetaldehyde = 1.0 ppb ppb^{-1}), but highest for Los Angeles (methanol = 21.7, acetone = 11.8, acetaldehyde = 5.4 ppb ppb^{-1}) (Brito et al., 2015 and references therein). The ERs of acetone and acetaldehyde estimated in this study are in the range of values for other cities and are comparable to those for Sao Paulo and London.

The ERs of OVOCs show larger variations compared to those of primary VOCs as reported for different urban sites of the world. The mixing ratios of OVOCs and benzene showed good correlations ($r^2 = 0.6\text{--}0.86$) at both sites. At the urban site, OVOCs are well correlated with traffic and combustion related emission tracers, such as benzene, toluene, and CO indicating their emissions from local anthropogenic (mostly vehicular) sources. The results obtained in the present and previous studies (e.g., Acton et al., 2020; Sahu et al., 2017; Tripathi & Sahu, 2020), suggest significantly higher contributions of anthropogenic sources than those from biogenic sources in the urban regions of south-east Asia during the winter season.

The good correlations of methanol with CO, toluene, and benzene at the suburban site indicate the dominant emissions from vehicles and combustion-related industrial sources. The higher background concentrations also indicate the contribution from regional biogenic and biomass burning sources in addition to anthropogenic sources. Consistently, a moderate correlation between methanol and isoprene ($r^2 = 0.58$) at the suburban site indicates the contribution of biogenic sources to some extent. A laboratory study of emission factors (EFs) of methanol from all major biogenic sources located in the study region will be important to quantify their contributions in ambient air. The ERs of $\Delta\text{methanol}/\Delta\text{benzene}$ were 2.4 ppb ppb^{-1} at the urban and 5.5 ppb ppb^{-1} at the suburban sites. However, the ERs of $\Delta\text{acetaldehyde}/\Delta\text{benzene}$ and $\Delta\text{acetone}/\Delta\text{benzene}$ do not show significant differences between the two sites. The strong correlations of OVOCs with both CO and benzene during the nighttime suggest that vehicular emissions are the main primary source at both sites. Previous studies have suggested that the ERs of $\Delta\text{OVOCs}/\Delta\text{CO}$ in ambient urban air are significantly higher than expected from vehicle exhaust (e.g., Borbon et al., 2013; Warneke et al., 2007). Karl et al. (2007) have reported the higher values of $\Delta\text{acetaldehyde}/\Delta\text{CO}$ ($\sim 11\text{ ppb ppb}^{-1}$) from tropical forest fires during the Tropical Forest and Fire Emission Experiment (TROFFEE) campaign in Brazil. A source apportionment study reported in our previous paper (Wang et al., 2020) explains the contributions from different emission sectors.

3.7. Daytime Ratios

The contributions from biogenic and photochemical sources can influence the VOC ratios with reference to a primary anthropogenic emission tracer. During the daytime (08–18 hr), the mixing ratios of isoprene and MTs showed stronger correlations with benzene at the urban site than those at the suburban site. The weaker correlations between acetone and benzene suggest a significant secondary formation of acetone at both sites. The higher slope of $\Delta\text{acetone}/\Delta\text{isoprene}$ during the daytime ($10.2 \text{ ppb ppb}^{-1}$) compared to the nighttime (7.2 ppb ppb^{-1}) at the urban site represents the secondary production of acetone during daytime (Figure 4b (i)). The slopes of $\Delta\text{acetone}/\Delta\text{isoprene}$ and their correlations for both day and nighttime are nearly the same at the suburban site (Figure 4b (iii)). In the daytime, mixing ratios of MVK + MACR and isoprene show strong correlations at the urban site but not at the suburban site (Figure 4b (ii) and (iv)). In summary, the weak correlations of isoprene and MTs with benzene at the suburban site and their strong correlations at the urban site during the daytime indicate a higher contribution from biogenic sources at the suburban site than at the urban site.

3.8. Variation of OVOCs With Photochemical Age

The determination of sources of ambient OVOCs in urban areas is challenging mainly due to their emissions from several types of sources such as fossil-fuel combustion, biomass/biofuel burning, and the use of volatile chemical products. In addition to direct emissions, the photo-oxidation of primary VOCs emitted from the vehicles can be a significant source of secondary VOCs and organic aerosols in urban regions (Robinson et al., 2007). Secondary organic compounds, including OVOCs, are formed from the photo-oxidation of VOCs emitted from both anthropogenic and biogenic sources (de Gouw et al., 2005; Hallquist et al., 2009). The contributions of primary sources to OVOCs have been estimated using their ratios to emission tracers (e.g., benzene and CO) (Inomata et al., 2010). The primary and secondary sources of different OVOCs were quantified using CO as a tracer of emissions at a surface site in Pasadena near Los Angeles, USA (de Gouw et al., 2018). In this study, we have calculated the photochemical age and used it as a reference to assess the oxidation processes leading to relative changes in the concentrations of OVOCs (Text S1 in Supporting Information S1). The photochemical age of an air mass can be determined using the ratios of two trace gases, mainly of reactive compounds such as VOCs (de Gouw et al., 2005). However, it is assumed that the pair of VOCs used to estimate the photochemical age have common emission sources and are removed mainly through their reactions with OH radicals at different rates. In this study, the mixing ratios of benzene and toluene were used to calculate the photochemical age because both sites are mainly influenced by vehicular emission. The photochemical age (t) is defined as the time-integrated exposure of an air mass to OH radicals (Kleinman et al., 2003).

$$t = \frac{1}{[\text{OH}](k_{\text{tol}} - k_{\text{benz}})} \left[\ln \left(\frac{T}{B} \right)_{t=0} - \ln \left(\frac{T}{B} \right)_{t=t} \right] \quad (3)$$

where k_{benz} ($1.22 \times 10^{-12} \text{ cm}^3 \text{ molecule}^{-1} \text{ s}^{-1}$) and k_{tol} ($5.36 \times 10^{-12} \text{ cm}^3 \text{ molecule}^{-1} \text{ s}^{-1}$) are the reaction rate constants of benzene and toluene with OH radicals (Atkinson & Arey, 2003). In this study, we have taken a mean OH concentration [OH] of $1 \times 10^6 \text{ molecule cm}^{-3}$, which has been used a standard value for the Asian outflow measured during the Intercontinental Chemical Transport Experiment (INTEX) campaign (Lelieveld et al., 2016; Mao et al., 2009). At the time of emission $(T/B)_{t=0}$ is the characteristic ratio of T/B . The $(T/B)_{t=0}$ values of 2.3 ppb ppb^{-1} for IITD and 2.5 ppb ppb^{-1} for MRIIRS were derived using the data measured during the early morning hours (00–05 hr), when emissions from HDVs were highest and impact of photochemical aging was lowest. However, the photochemical age estimated using the VOC ratio method has several limitations related to the transport and mixing of air masses from distinct sources with different ages (McKeen & Liu, 1993). The emissions from HDVs are a significant source of many NMHCs but particularly of aromatic VOCs (benzene and toluene) (Sawyer et al., 2000). The OH radicals oxidize the NMHCs emitted from vehicles during the night to early morning period in the daytime. To some extent, OVOCs/CO ratios account for other factors such as the meteorological parameters and PBL dynamics, which can change the concentrations of OVOCs. Nevertheless, to investigate the photochemical evolution of vehicular exhaust and to exclude the inferences of aged background air masses and fresh emissions, we have divided the data based on low NO ($<4 \text{ ppbv}$), moderate NO ($4\text{--}20 \text{ ppbv}$), and high NO ($>20 \text{ ppbv}$) values.

At the urban site, under moderate NO concentrations, the average acetone/CO, acetaldehyde/CO, MEK/CO, and MVK + MACR/CO ratios increased rapidly from 6, 6, 1.1, and $0.17 \text{ ppb ppm}^{-1}$ to 9, 8, 1.5, and $0.32 \text{ ppb ppm}^{-1}$,

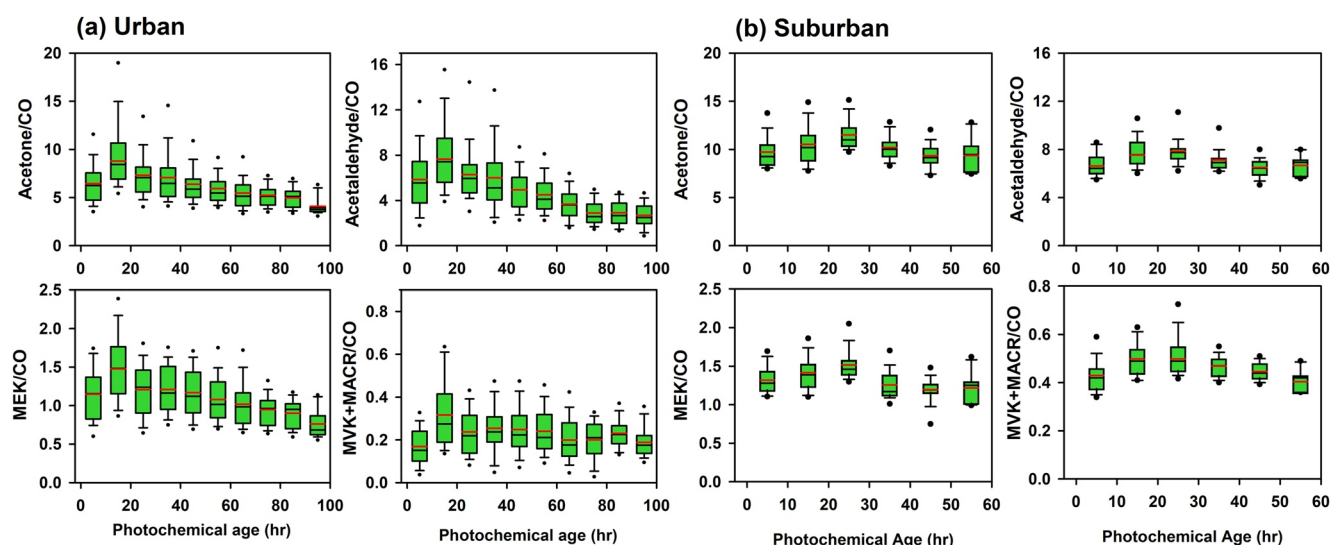


Figure 8. The box whisker plots showing the dependencies of OVOC/CO (ppb ppm⁻¹) ratios on the photochemical age at (a) IITD urban and (b) MRIIRS suburban sites in New Delhi during the winter season 2018.

respectively, in the initial stages of photochemical aging (0–15 hr). However, the ratios decreased gradually in the air masses with higher photochemical ages (>20 hr) (Figure 8a). At this site, the OVOCs/CO ratios measured under low and high NO concentrations do not exhibit any apparent dependence on the photochemical age (Figure S8a and Text S2 in Supporting Information S1). At the suburban site, under moderate NO concentrations, the acetone/CO, acetaldehyde/CO, MEK/CO, and MVK + MACR/CO ratios increased gradually from ~10, 7, 1.3, and 0.4 ppb ppm⁻¹ to ~12, 8, 1.5, and 0.5 ppb ppm⁻¹, respectively, at lower photochemical ages (0–25 hr). However, the ratios decreased in the air masses at higher photochemical ages (Figure 8b). The ratios do not exhibit any clear relations with the photochemical age at low and high NO concentrations (discussed in Text S2 and Figure S8b in Supporting Information S1).

At moderate NO concentrations, the increasing and decreasing ratios of OVOCs/CO indicate the predominant photochemical production and loss of OVOCs, respectively. Overall, the enhancements of OVOCs/CO between the two sites show different relationships with photochemical age. de Gouw et al. (2005) have reported the increase of secondary contributions to OVOCs in moderately aged air masses compared to those in more aged air masses during the New England Air Quality Study (NEAQS) 2002. The suburban site (downwind) represent the measurements of more aged air masses with higher contributions of OVOCs from secondary/biogenic sources than those at the urban site. As shown in the diurnal plots (Figure 7), the enhancements of OVOCs/benzene ratios in the afternoon hours at the suburban site indicate higher contributions from secondary sources than those at the urban site. The transport time of plumes from upwind regions could cause the delay in peaks of OVOCs/CO at the suburban site in reference to those at the urban site. As a result, the increase of OVOCs/CO extended up to 25 hr of photochemical aging at the suburban site. The influences of anthropogenic emissions from vehicular and other sources in the daytime are higher at the urban site than those at the suburban site. Therefore, it is complex to track the photochemical transformation of air masses leading to the secondary formation of OVOCs at the urban site.

3.9. Estimates of Anthropogenic and Biogenic/Secondary Contributions

In urban and suburban areas, the separation of contributions of different sources to ambient VOCs is difficult due to the complex source and sink processes. The contributions of primary and secondary (photochemical) sources to ambient VOCs can be separated and quantified using CO or benzene as a tracer of primary emissions (e.g., de Gouw et al., 2018). A source-tracer-ratio method has been widely used to separate the contributions of anthropogenic, biogenic/secondary sources of VOCs (e.g., Legreid et al., 2007; Yuan et al., 2012). Anthropogenic contributions can be estimated using the following relation between ERs of OVOCs, isoprene, and MTs with reference to CO derived using nighttime (0–5 hr) data (Bon et al., 2011; Borbon et al., 2013).

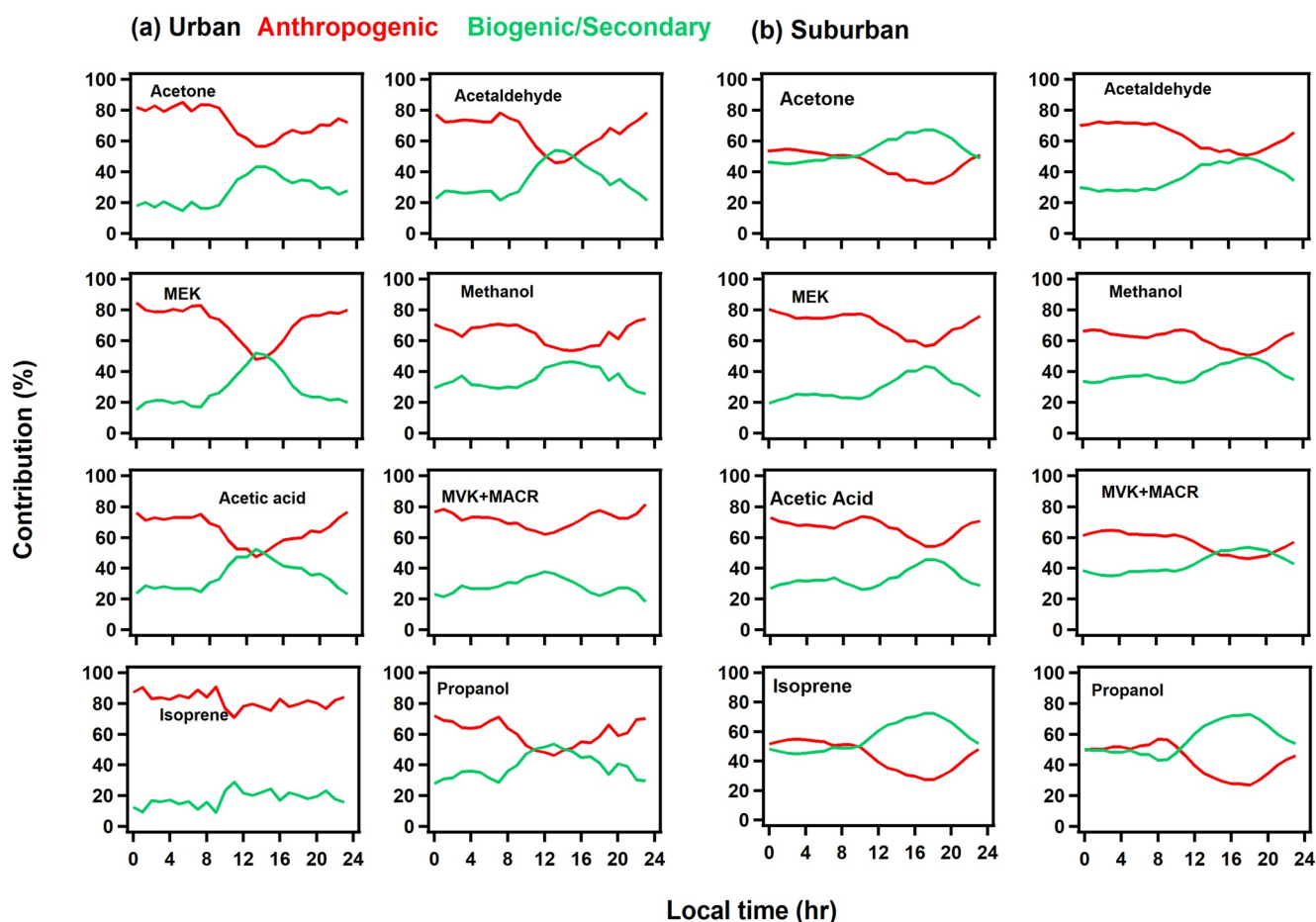


Figure 9. The percentage contributions of biogenic/secondary and anthropogenic sources to the ambient mixing ratios of different VOCs at (a) IITD urban and (b) suburban sites in New Delhi during the winter season 2018.

$$\text{Anthropogenic VMR of VOC} = ER \times \text{VMR of CO} \quad (4)$$

where *VMR* stands for the volume mixing ratio of a given compound. The anthropogenic contribution to ambient mixing ratio of a VOC can be calculated by assuming that both sites were mainly influenced by combustion-related sources such as vehicle exhaust and residential/commercial fossil fuel use. While non-combustion anthropogenic sources of VOCs (such as industrial and evaporative emissions) are not considered here. The non-anthropogenic contribution is dominated by biogenic and/or secondary sources in the urban atmosphere (Brito et al., 2015). Therefore, the contribution of biogenic and/or secondary sources to ambient mixing ratio of a VOC can be estimated by the following equation.

$$\text{Biogenic/Secondary VMR of VOC} = \text{VMR} - \text{Anthropogenic VMR of VOC} \quad (5)$$

The average diurnal percentage contributions of primary anthropogenic and biogenic/secondary sources to ambient air mixing ratios of OVOCs and isoprene are shown in Figure 9. At the urban site, the biogenic/secondary sources show higher contributions in the daytime with peak values around noon. The average contributions of anthropogenic sources to ambient isoprene, acetone, methanol, propanol, MEK, and MVK + MACR mixing ratios are estimated to be $82 \pm 5\%$, $73 \pm 9\%$, $65 \pm 7\%$, $61 \pm 8\%$, $72 \pm 5\%$, and $72 \pm 11\%$, respectively (Figure 9a). During nighttime and early morning, anthropogenic sources made much higher contributions to mixing ratios of almost all VOCs at both sites. The contributions of secondary sources to acetic acid, acetaldehyde, MEK, and propanol reached $\sim 50\%$ during the daytime. The fractions of non-anthropogenic (biogenic) isoprene ($\sim 18\%$) are significantly smaller than those ($>25\%$) estimated for OVOCs from biogenic and/or secondary sources.

Therefore, in addition to their biogenic emissions, the differences in non-anthropogenic contributions of isoprene and OVOCs indicate significant secondary formations of OVOCs.

The contributions of biogenic/secondary sources at the suburban site are estimated to be higher than those for the urban site (Figure 9b). As expected, the biogenic/secondary fractions of VOCs are higher in the daytime with peak values during the afternoon-evening hours. In the daytime, the average percentage contributions of biogenic sources to ambient air isoprene at the suburban site were ~61%. While the contributions of biogenic/secondary sources to OVOCs including acetic acid and MVK + MACR reached 40%–50% in the daytime (Figure 9b). Overall, the total average percentage contributions of biogenic/secondary sources to OVOCs and isoprene are estimated to be 30%–57% and ~57%, respectively. The emissions of precursors from primary anthropogenic and biogenic sources could have resulted in the higher abundances of secondary OVOCs at the suburban site. The reduction in traffic-related emissions is another factor leading to the decrease of anthropogenic contributions in the daytime. However, the estimates of the biogenic/secondary contributions during the day are subject to considerable uncertainty primarily due to the use of CO as a tracer for all anthropogenic emissions. The estimated biogenic/secondary contributions to OVOCs and BVOCs should be considered a lower limit as VOCs + OH reaction rates are higher than CO + OH ($2.7 \times 10^{-13} \text{ cm}^3 \text{ molecule}^{-1} \text{ s}^{-1}$) rate (Butler et al., 1978; Cox et al., 1976).

Sahu, Yadav, and Pal (2016) have reported relatively low anthropogenic contributions to ambient average mixing ratios of isoprene ($63 \pm 12\%$), acetone ($44 \pm 7\%$), and acetaldehyde ($44 \pm 6\%$) at an urban site of Ahmedabad in western India for the winter season. The results are consistent as primary anthropogenic sources had higher contributions due to less secondary production and lower biogenic emissions in winter. At Beijing in China, anthropogenic contributions to ambient air isoprene, acetone, and acetaldehyde were estimated to be ~94, 86%, and 79%, respectively during the haze period in winter (Sheng et al., 2018). In addition to different emissions sources, the different meteorological conditions could explain the differences in contributions from primary and secondary sources in these cities. For example, the average temperatures at Ahmedabad, Beijing, and New Delhi were ~24, <10, and 16°C during the respective study periods in the winter season. In addition to different meteorological and environmental conditions, the differences in local biogenic sources (vegetation) among these urban regions could also lead to varying contributions from biogenic/secondary sources.

3.10. OH Reactivity and Ozone Formation Potential (OFP)

The overall sink of OH in a given environment can be characterized by the measure of total OH reactivity, which is the total loss rate of OH or inverse of OH lifetime (s^{-1}) (Bsaibes et al., 2020; Williams & Brune, 2015). The OH reactivity of VOCs can be used to assess their impact on atmospheric chemistry in different environments. However, the total measured and the calculated OH reactivity often show significant differences indicating unquantified OH loss known as the missing sinks (Yang et al., 2016). In this study, we have calculated the OH reactivity of dominant VOCs, NO and NO₂ measured at both the sites using Equation S7 (Text S3 in Supporting Information S1). Instead of characterizing their contribution to the total OH reactivity, our main objective is to compare their contributions to the urban and suburban sites of New Delhi.

We have calculated the OH reactivity of dominant VOCs, NO and NO₂ measured at both sites using Equation S7 (Text S3 in Supporting Information S1). The OH reaction rates of NO₂ and NO are $1.2 \times 10^{-11} \text{ cm}^3 \text{ molecule}^{-1} \text{ s}^{-1}$ (Atkinson et al., 2004) and $9.7 \times 10^{-12} \text{ cm}^3 \text{ molecule}^{-1} \text{ s}^{-1}$ (Wang et al., 2021) at 298 K, respectively. The total OH reactivity at the urban site (70 s^{-1}) during the nighttime is about 2.5 times higher than the reactivity at the suburban site ($\sim 27 \text{ s}^{-1}$). At the urban site, the average contributions to OH reactivity by aromatics, OVOCs, isoprene, MTs, NO and NO₂ to OH reactivity were ~4, 8%, 5%, 0.4%, 45%, and 36%, respectively (Figure S9 in Supporting Information S1). At the suburban site, the average contributions of aromatic, OVOCs, isoprene, MTs, NO and NO₂ to OH reactivity were ~7, 13%, 24%, 4%, 5%, and 16%, respectively. The reactivity values of NO and NO₂ at the urban site were higher than those at the suburban site. The large local variations in the composition of VOCs and other trace gases result in significant differences in the total OH reactivity between the urban and suburban sites. The emissions of NO from vehicular sources especially from HDVs are higher at the urban site (average > 100 ppbv) than those at the suburban site (average ~10 ppbv). The level of OH reactivity at the suburban site is higher in January than in February and March. The mean OH reactivity of isoprene at the suburban site in January (10 s^{-1}) was higher than the values ($\sim 6 \text{ s}^{-1}$) determined for March, while values were nearly the same for all three months at the urban site. As shown in Figure 10, relatively large diurnal variations of OH reactivity at the urban site seem to be governed by the pronounced day and night differences in the mixing ratios of NO

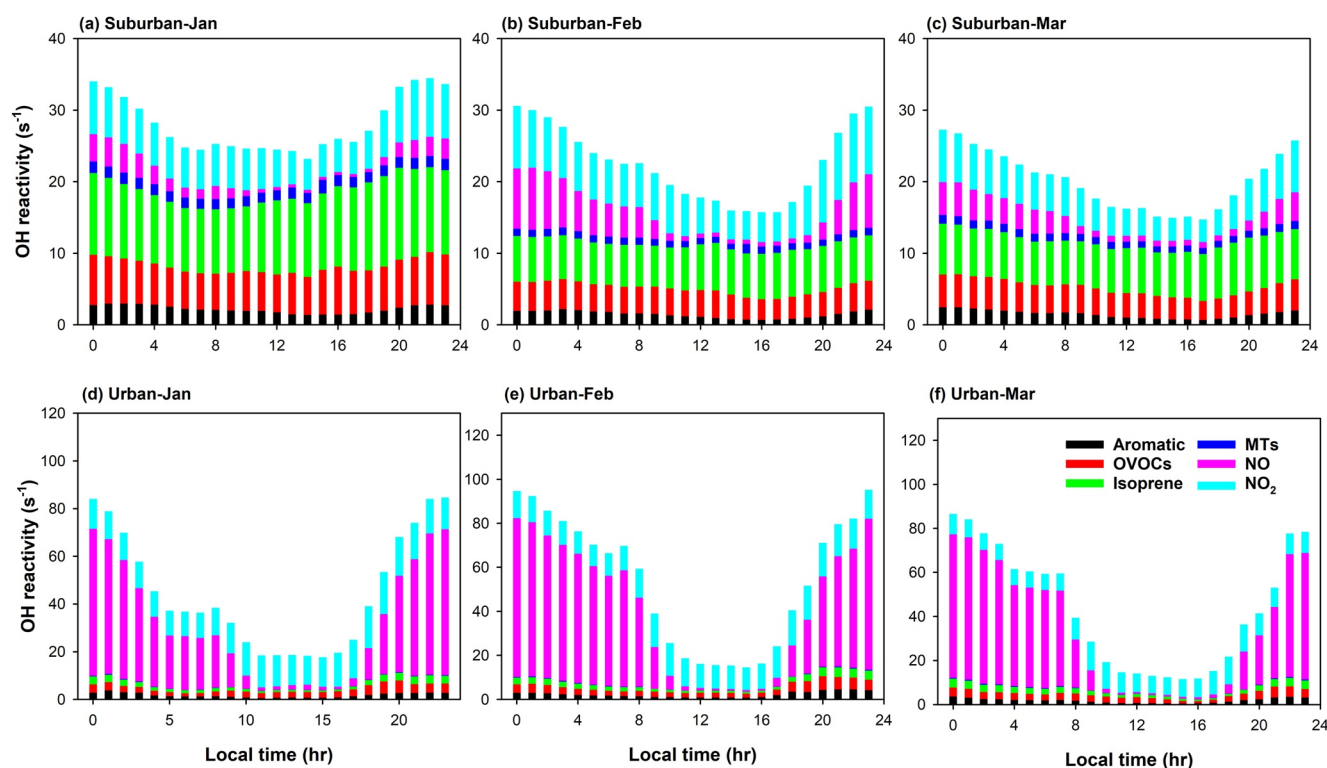


Figure 10. The mean diurnal OH reactivity of OVOCs, aromatics, isoprene, MTs, NO, and NO₂ at the suburban (a–c) and at urban (d–f) sites in New Delhi during different months in the winter of 2018.

and NO₂. The average OH reactivity of NO (>60 s^{−1}) at the urban site at midnight is higher than the daytime values of ~1 s^{−1}. The higher reactivity of isoprene in the suburban region has been mainly attributed to biogenic sources. The total OH reactivity at the suburban site is similar to the values reported for Beijing, China (Williams et al., 2016), but the compound-specific contributions are different. Like Beijing, the contributions of NO and NO₂ to the OH reactivity are much higher compared to isoprene at the urban site in New Delhi.

Despite the reductions of isoprene and OVOC reactivity due to deeper PBL, the greater contribution of secondary/biogenic sources in March seems to balance it out. Therefore, in addition to the emission and chemical production/loss processes, the variation of PBL depth is important in controlling the reactivity. The PBL heights affect the mixing ratios of VOCs, which in turn affect the ROH values (Gilman et al., 2009).

The photochemical formation of O₃ in the troposphere depends on several factors such as the reactivity of VOCs, NO_x concentration, and meteorological conditions (Tan et al., 2012). Typically, in the high NO_x regimes, the rate of O₃ formation is controlled by the levels of radicals produced by the oxidations of VOCs. However, in the lower NO_x regimes, the level of NO_x controls the formation of O₃ (Carter, 1994). The concentration-based representation of VOCs is simple, but it has a disadvantage in assessing their sensitivities to the formation of O₃ and SOA. Alternatively, several reactivity-based approaches have been used to assess the importance of different VOCs in the formation of O₃. The two main approaches are the Propylene-Equivalent (Propy–Equiv) concentration (PEC) described by Chameides et al. (1992) and the OFP (Carter, 1994) (Equation S8 and S9 in Supporting Information S1). We have calculated OFP values of different VOCs using the *MIR* values reported in Carter (1994) using Equation S8 (Text S4 in Supporting Information S1). The OFP values of different VOCs for January, February, and March are shown in Figure 11. The OFP values of almost all VOCs at the urban site are higher than their value at the urban site mainly due to the higher concentration of VOCs. Among VOCs presented in this study, each of xylenes, acetaldehyde and isoprene accounted for 22%–25%, followed by toluene (10%) to the sum of OFPs at the suburban site. At the urban site, the OFP values for xylenes, toluene, acetaldehyde and isoprene were significantly higher than those for other VOCs (Figure 11). Nonetheless, other factors such as the NO_x level and

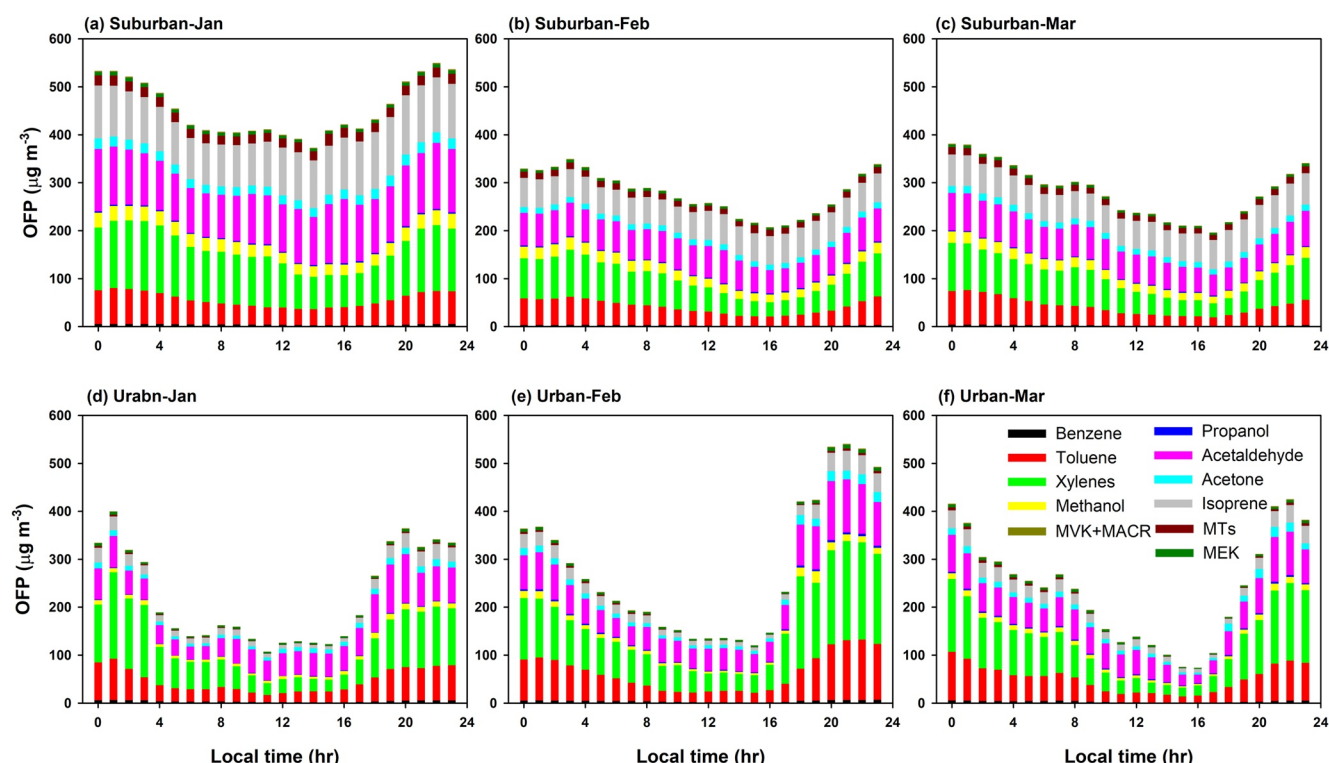


Figure 11. The mean diurnal plots of the ozone formation potential (OFP) of different VOCs at the MRIIRS suburban (a–c) and IITD urban (d–f) sites in New Delhi during different months in the winter of 2018.

solar radiation intensity also affect the production of O_3 in the troposphere (Tan et al., 2012). In reality, the interpretation using OFP or PEC does not fully explain how VOCs influence O_3 chemistry.

3.11. Sensitivity of VOCs and NO_x on Ozone Formation

The ground-level formation of O_3 is sensitive to both VOCs and NO_x concentrations in urban settings (Mazzuca et al., 2016). Understanding O_3 production/loss is a significant challenge in comprehending the non-linear chemistry with its precursors such as VOCs, NO_x , and VOCs/ NO_x ratios. The O_3 production can be either VOC-sensitive, NO_x -sensitive or both (VOCs as well NO_x) due to the complexity of photochemical processes. The sensitivity of O_3 production to VOCs and NO_x represents a considerable uncertainty for oxidant photochemistry in urban areas (Sillman et al., 2003). In the present study, we performed simulations using a photochemical box model to investigate the O_3 production variations in VOCs and NO_x levels at the two study sites in New Delhi.

The levels of NO_x and VOCs were adjusted iteratively (Chen et al., 2021) for the base case to simulate the diurnal cycles of O_3 measured at both sites during the study period (Figures 12 and 13). A series of sensitivity simulations have been conducted to analyze the non-linear VOC- NO_x - O_3 relationship in these urban and suburban environments. Two sets of sensitivity simulations were performed for each site, one with varying NO_x and the other with varying VOCs. For the base scenario in the model, the NO_x levels are 55 and 122 ppbv over the suburban and urban sites, respectively. Total VOCs (species mentioned in Table 1 + NMHCs) are 198 and 446 ppbC for the suburban and urban sites, respectively for the base scenario in the model. In agreement with the observations at the suburban site, the model (base run) tends to reproduce the O_3 build-up around noontime. However, during the nighttime, the simulated O_3 mixing ratios show a significant difference compared to observations. Overall, except for the evening period (17–18 hr), the mixing ratios of O_3 simulated with adjusted NO_x (–20% to 50%) and VOCs (–50% to 50%) from the base case condition agree with the observed (average \pm standard deviation) values (Figure 12). In Figure 12a, the total VOC value is fixed at 198 ppbC and NO_x is varied from 27 ppbv (–50% NO_x simulation) to 110 ppbv (+100% NO_x simulation). Similarly, in Figure 12b, NO_x is fixed at 55 ppbv and the total VOC is varied from 99 ppbC (–50% VOCs simulation) to 396 ppbC (+100% VOCs simulation). The difference

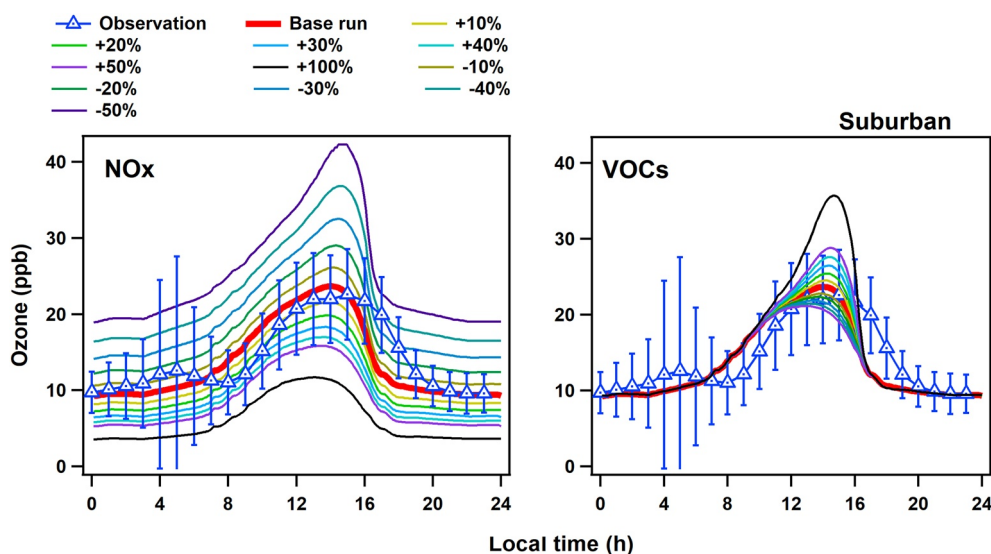


Figure 12. Box-model simulated diurnal variations of O_3 for different NO_x levels with fixed VOCs (left panel) and different VOC levels with fixed NO_x (right panel) at the suburban site (MRIIRS). The average diurnal variation of O_3 measured during the study period (10 January to 7 March 2018) is also shown for comparison.

between observation and model simulation can be attributed mainly to the unaccounted transport effect in the box model. The differences between the simulated and observed mixing ratios of O_3 , including underestimated night levels, are consistent with a recent study for this environment (Chen et al., 2021). Ozone measurements could not be made at the urban site (Figure 13) to compare with model simulation. Nevertheless, the model is shown to reproduce contrasting chemical environments for the suburban site here and other stations in the Indian region in earlier studies (Ojha et al., 2012; Soni et al., 2021). At the suburban site, the maximum net O_3 production rate for base simulation is ~ 4 ppbv hr^{-1} , which increases to 7.5 ppbv hr^{-1} in +50% VOCs scenario. Whereas, O_3 production rate decreases to 1.1 ppbv hr^{-1} in +50% NO_x case. Even though O_3 levels are lower at the suburban site, the result that O_3 level is enhanced by VOCs (but saturated by NO_x) is in agreement with another station in the Delhi region (Nelson et al., 2021). The model consists of important isoprene reactions with for example, NO_3 , O_3 , and OH (Calvert et al., 2008). The sensitivity simulations suggest that isoprene could enhance maximum

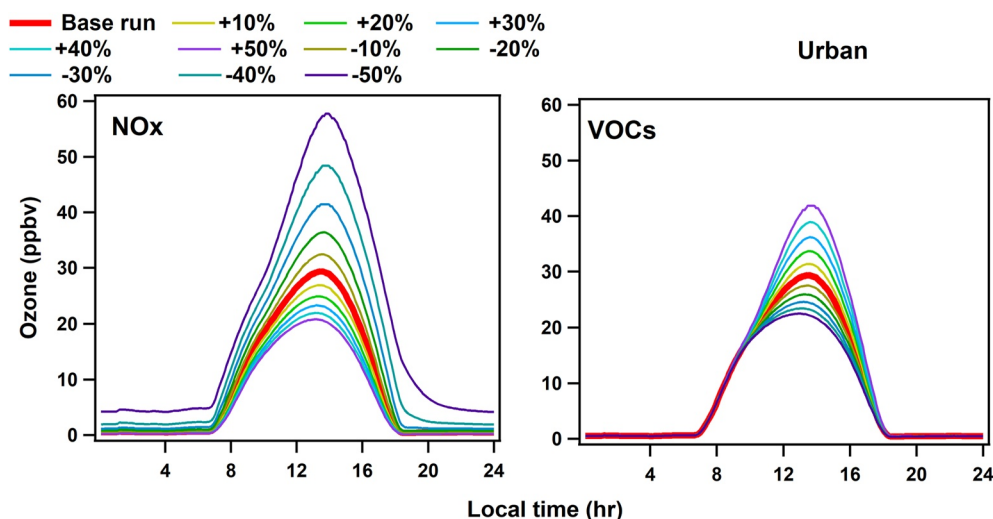


Figure 13. Box-model simulated diurnal variation of O_3 mixing ratio at urban site (IITD). In addition to the base run, simulations of O_3 for different NO_x levels with fixed VOCs (left) and different VOC levels with fixed NO_x (right) are shown.

noontime O₃ by 2.4 ppbv (10.4%) at the suburban site. The contribution was estimated to be smaller (2.2%) at the urban site.

Noticeably, the O₃ mixing ratio build-up around the noontime increased with the increasing VOC concentrations at both sites. At the suburban site, the changes in O₃ mixing ratios were in the ranges of −7 to 20 ppbv and −3 to 7 ppbv for the simulations within $\pm 50\%$ changes of both NO_x (with fix VOCs) and VOCs (with fix NO_x), respectively. Simulations also show that the strong VOC enhancements (+100%) with fixed NO_x can enhance O₃ levels beyond the observed day-to-day variability.

Qualitatively, this finding based on detailed chemistry driven by observations agrees with the results reported using simplified chemistry in a regional chemical transport model (Sharma et al., 2017). This sensitivity analysis, especially during the afternoon, indicates that the NO_x-saturated or VOC-sensitive regime controls the O₃ photochemistry at both sites. It is suggested that reductions in local VOC emissions would help reduce photochemical O₃ build-up over Delhi and its downwind regions. However, as the IGP region is shown to be strongly impacted by the transport from upwind regions, also from outside India (David & Ravishankara, 2019), emission reductions over larger regions would be necessary to improve the air quality over Delhi.

4. Conclusion

Ambient mixing ratios of VOCs were measured using the PTR-TOF-MS instruments at the urban and suburban sites of New Delhi in India during the winter season of 2018. The day-to-day and diurnal variations in the concentration and composition of VOCs were caused by the changes in vehicular emissions, meteorological conditions, and episodic plumes from biomass burning and industrial sources. Typically, the higher and lower levels of VOCs were measured during calm and stronger winds, respectively. The composition of VOCs and their strong correlations with CO and benzene during the nighttime indicate the dominance of vehicular emissions at both sites. The average mixing ratios of aromatic VOCs were comparable at both sites, while OVOCs and BVOCs were significantly higher at the suburban site. The strong correlations of VOCs with CO, acetonitrile, furfural, furan indicate the influences of biomass/wood burning, particularly during the *Holi* festival. However, in some cases, the time series trend of acetonitrile (a tracer of biomass burning) does not follow CO, indicating additional contributions from industrial and chemical sources. The higher levels of VOC/CO ratios measured in moderately aged air masses at both sites elucidate the net secondary formation of OVOCs. $\Delta\text{VOC}/\Delta\text{CO}$ emission ratios were used to estimate contributions of primary anthropogenic and biogenic/secondary sources. The average percentage contributions of anthropogenic sources to OVOCs and isoprene were 60%–73%, and 82% at the urban site, while these were 40%–70%, and 43% at the suburban site, respectively. The daytime contributions of biogenic/secondary sources to ambient air mixing ratios of OVOCs, isoprene, and MTs at the suburban site were significantly higher than those at the urban site. Model simulations suggest that limiting the emissions of VOCs is important since the reductions in NO_x alone do not yield mitigation of O₃ pollution and instead further increase ozone in the environment of Delhi.

The results presented in this study suggest the need for developing emission inventories of speciated VOCs from different sectors. A detailed understanding of the emission and photochemical processes of VOCs is required to accurately model the variations of secondary pollutants such as O₃ and SOA. Further, it is also important to investigate the contributions of different sources and compositions of VOCs in other seasons. The continuous measurements of various anthropogenic and biogenic VOCs are required throughout the year, which will help in planning the control strategies for the air quality improvements in New Delhi and other parts of the polluted Indo-Gangetic plain. The measurement-based studies of VOCs need greater attention to investigate the regional importance of biogenic and photochemical processes in South Asia.

Conflict of Interest

The authors declare no conflicts of interest relevant to this study.

Data Availability Statement

Data: The data (VOCs, CO, NO_x, and O₃) used in this study are archived at a public data repository at Figshare <https://doi.org/10.6084/m9.figshare.12496169.v2> (Tripathi et al., 2021). The photochemical box model simulations were performed using the NCAR Master Mechanism (Madronich et al., 2006; Chen et al., 2021) version-2.5. We used ECMWF (Hersbach et al., 2018) for PBL and underground for weather parameters (Weather Underground, 2018). **Software:** Figures were made with Matlab 2019 (MATLAB, 2019), Sigma Plot 14 (SigmaPlot, 2018), and IGOR Pro 6.37 (IGOR, 2016).

Acknowledgments

Nidhi Tripathi and L. K. Sahu acknowledge Prof. Anil Bhardwaj, Director, Physical Research Laboratory (PRL), Ahmedabad, India, for the support and permission to deploy the PRL PTR-TOF-MS instrument for the experimental campaign. The authors gratefully acknowledge the ECMWF for PBL and weather underground archive for weather data. We are thankful to Sasha Madronich and co-workers for the availability of the NCAR Master Mechanism model through the NCAR ACOM website. The authors would like to thank Mr. Ashok from MARS Bio Analytical, New Delhi, for their support during the campaign. Nidhi Tripathi is thankful to Ms. Sourita Saha for her support in data analysis. Sachchida N. Tripathi gratefully acknowledges the financial support provided by the Department of Biotechnology (DBT), Government of India to conduct this research under Grant No. BT/IN/UK/APHH/41/KB/2016-17 dated 19 July 2017 and financial support provided by the Central Pollution Control Board (CPCB), Government of India to conduct this research under Grant No. 495 AQM/Source apportionment EPC Project/2017. The contribution by the Swiss National Science Foundation project 200021_169787. Source Apportionment of Organics in ambient air including Primary, Secondary Organic Aerosols and trace Gases (SAOPSOAG) is acknowledged.

References

- Acton, W. J. F., Huang, Z., Davison, B., Drysdale, W. S., Fu, P., Hollaway, M., et al. (2020). Surface-atmosphere fluxes of volatile organic compounds in Beijing. *Atmospheric Chemistry and Physics*, 20(23), 15101–15125. <https://doi.org/10.5194/acp-20-15101-2020>
- Akagi, S., Yokelson, R. J., Wiedinmyer, C., Alvarado, M., Reid, J., Karl, T., et al. (2011). Emission factors for open and domestic biomass burning for use in atmospheric models. *Atmospheric Chemistry and Physics*, 11(9), 4039. <https://doi.org/10.5194/acp-11-4039-2011>
- Anenberg, S. C., Horowitz, L. W., Tong, D. Q., & West, J. J. (2010). An estimate of the global burden of anthropogenic ozone and fine particulate matter on premature human mortality using atmospheric modeling. *Environmental Health Perspectives*, 118(9), 1189–1195. <https://doi.org/10.1289/ehp.0901220>
- Atkinson, R., & Arey, J. (2003). Atmospheric degradation of volatile organic compounds. *Chemical Reviews*, 103(12), 4605–4638. <https://doi.org/10.1021/cr0206420>
- Atkinson, R., Baulch, D., Cox, R., Crowley, J., Hampson, R., Hynes, R., et al. (2004). Evaluated kinetic and photochemical data for atmospheric chemistry: Volume I-gas phase reactions of Ox, HOx, NOx and SOx species. *Atmospheric Chemistry and Physics*, 4(6), 1461–1738.
- Baker, A., Schuck, T., Slemr, F., Van Velthoven, P., Zahn, A., & Brenninkmeijer, C. (2011). Characterization of non-methane hydrocarbons in Asian summer monsoon outflow observed by the CARIBIC aircraft. *Atmospheric Chemistry and Physics*, 11(2), 503. <https://doi.org/10.5194/acp-11-503-2011>
- Bon, D., Ulbrich, I., De Gouw, J., Warneke, C., Kuster, W., Alexander, M., et al. (2011). Measurements of volatile organic compounds at a suburban ground site (T1) in Mexico City during the MILAGRO 2006 campaign: Measurement comparison, emission ratios, and source attribution. *Atmospheric Chemistry and Physics*, 11(6), 2399–2421. <https://doi.org/10.5194/acp-11-2399-2011>
- Borbon, A., Gilman, J., Kuster, W., Grand, N., Chevaillier, S., Colomb, A., et al. (2013). Emission ratios of anthropogenic volatile organic compounds in northern mid-latitude megacities: Observations versus emission inventories in Los Angeles and Paris. *Journal of Geophysical Research: Atmospheres*, 118(4), 2041–2057. <https://doi.org/10.1002/jgrd.50059>
- Brito, J., Wurm, F., Yáñez-Serrano, A. M., De Assunção, J. V., Godoy, J. M., & Artaxo, P. (2015). Vehicular emission ratios of VOCs in a megacity impacted by extensive ethanol use: Results of ambient measurements in Sao Paulo, Brazil. *Environmental Science & Technology*, 49(19), 11381–11387. <https://doi.org/10.1021/acs.est.5b03281>
- Brunamonti, S., Füzér, L., Jorge, T., Poltera, Y., Oelsner, P., Meier, S., et al. (2019). Water vapor in the Asian summer monsoon anticyclone: Comparison of balloon-borne measurements and ECMWF data. *Journal of Geophysical Research: Atmospheres*, 124(13), 7053–7068. <https://doi.org/10.1029/2018jd030000>
- Bruns, E. A., ElHaddad, I., Slowik, J. G., Kilic, D., Klein, F., Baltensperger, U., & Prévôt, A. S. (2016). Identification of significant precursor gases of secondary organic aerosols from residential wood combustion. *Scientific Reports*, 6, 27881. <https://doi.org/10.1038/srep27881>
- Bruns, E. A., Slowik, J. G., ElHaddad, I., Kilic, D., Klein, F., Dommen, J., et al. (2017). Characterization of gas-phase organics using proton transfer reaction time-of-flight mass spectrometry: Fresh and aged residential wood combustion emissions. *Atmospheric Chemistry and Physics*, 17(1), 705–720. <https://doi.org/10.5194/acp-17-705-2017>
- Bsaibes, S., Al Ajami, M., Mermet, K., Truong, F., Batut, S., Hecquet, C., et al. (2020). Variability of hydroxyl radical (OH) reactivity in the Landes maritime pine forest: Results from the LANDEX campaign 2017. *Atmospheric Chemistry and Physics*, 20(3). <https://doi.org/10.5194/acp-20-1277-2020>
- Butler, R., Solomon, I., & Snelson, A. (1978). Rate constants for the reaction of OH with halocarbons in the presence of O₂ + N₂. *Journal of the Air Pollution Control Association*, 28(11), 1131–1133. <https://doi.org/10.1080/00022470.1978.10470717>
- Bylinski, H., Barczak, R. J., Gębicki, J., & Namieśnik, J. (2019). Monitoring of odors emitted from stabilized dewatered sludge subjected to aging using proton transfer reaction-mass spectrometry. *Environmental Science and Pollution Research International*, 26(6), 5500–5513. <https://doi.org/10.1007/s11356-018-4041-4>
- Calvert, J. G., Derwent, R. G., Orlando, J. J., Wallington, T. J., & Tyndall, G. S. (2008). *Mechanisms of atmospheric oxidation of the alkanes*. Oxford University Press (ISBN: 978-0-19-536581-8). Received from <https://books.google.de/books?id=uWoSDAAQBAJ>
- Carter, W. P. (1994). Development of ozone reactivity scales for volatile organic compounds. *Air & Waste*, 44(7), 881–899. <https://doi.org/10.1080/1073161x.1994.10467290>
- Chameides, W., Fehsenfeld, F., Rodgers, M., Cardelino, C., Martinez, J., Parrish, D., et al. (1992). Ozone precursor relationships in the ambient atmosphere. *Journal of Geophysical Research: Atmospheres*, 97(D5), 6037–6055. <https://doi.org/10.1029/91jd03014>
- Chandra, N., Lal, S., Venkataramani, S., Patra, P. K., & Sheel, V. (2016). Temporal variations of atmospheric CO₂ and CO at Ahmedabad in western India. *Atmospheric Chemistry and Physics*, 16(10), 6153–6173. <https://doi.org/10.5194/acp-16-6153-2016>
- Chen, Y., Beig, G., Archer-Nicholls, S., Drysdale, W., Acton, W. J. F., Lowe, D., et al. (2021). Avoiding high ozone pollution in Delhi, India. *Faraday Discussions*, 226, 502–514. <https://doi.org/10.1039/D0FD00079E>
- Chutia, L., Ojha, N., Girach, I. A., Sahu, L. K., Alvarado, L. M., Burrows, J. P., et al. (2019). Distribution of volatile organic compounds over Indian subcontinent during winter: WRF-chem simulation versus observations. *Environmental Pollution*, 252, 256–269. <https://doi.org/10.1016/j.envpol.2019.05.097>
- Coggon, M. M., Veres, P. R., Yuan, B., Koss, A., Warneke, C., Gilman, J. B., et al. (2016). Emissions of nitrogen-containing organic compounds from the burning of herbaceous and arboraceous biomass: Fuel composition dependence and the variability of commonly used nitrile tracers. *Geophysical Research Letters*, 43(18), 9903–9912. <https://doi.org/10.1002/2016gl070562>
- Cox, R. A., Derwent, R. G., & Holt, P. M. (1976). Relative rate constants for the reactions of OH radicals with H₂, CH₄, CO, NO and HONO at atmospheric pressure and 296 K. *Journal of the Chemical Society, Faraday Transactions: Physical Chemistry in Condensed Phases*, 72, 2031–2043. <https://doi.org/10.1039/f1976202031>

- Dave, P. N., Sahu, L. K., Tripathi, N., Bajaj, S., Yadav, R., & Patel, K. (2020). Emissions of non-methane volatile organic compounds from a landfill site in a major city of India: Impact on local air quality. *Heliyon*, 6(7), e04537. <https://doi.org/10.1016/j.heliyon.2020.e04537>
- David, L. M., & Ravishankara, A. (2019). Boundary layer ozone across the Indian subcontinent: Who influences whom? *Geophysical Research Letters*, 46(16), 10008–10014. <https://doi.org/10.1029/2019gl082416>
- David, L. M., Ravishankara, A., Brewer, J. F., Sauvage, B., Thouret, V., Venkataramani, S., & Sinha, V. (2019). Tropospheric ozone over the Indian subcontinent from 2000 to 2015: Data set and simulation using GEOS-Chem chemical transport model. *Atmospheric Environment*, 219, 117039. <https://doi.org/10.1016/j.atmosenv.2019.117039>
- De Gouw, J., Gilman, J., Kim, S., Alvarez, S., Dusanter, S., Graus, M., et al. (2018). Chemistry of volatile organic compounds in the Los Angeles Basin: Formation of oxygenated compounds and determination of emission ratios. *Journal of Geophysical Research: Atmospheres*, 123(4), 2298–2319. <https://doi.org/10.1002/2017jd027976>
- De Gouw, J., Middlebrook, A., Warneke, C., Goldan, P., Kuster, W., Roberts, J., et al. (2005). Budget of organic carbon in a polluted atmosphere: Results from the new England air quality study in 2002. *Journal of Geophysical Research: Atmospheres*, 110(D16). <https://doi.org/10.1029/2004JD005623>
- De Gouw, J., Warneke, C., Scheeren, H., Van Der Veen, C., Bolder, M., Scheele, M., et al. (2001). Overview of the trace gas measurements on board the Citation aircraft during the intensive field phase of INDOEX. *Journal of Geophysical Research: Atmospheres*, 106(D22), 28453–28467. <https://doi.org/10.1029/2000jd900810>
- De Gouw, J., Welsh-Bon, D., Warneke, C., Kuster, W., Alexander, L., Baker, A. K., et al. (2009). Emission and chemistry of organic carbon in the gas and aerosol phase at a sub-urban site near Mexico City in March 2006 during the MILAGRO study. *Atmospheric Chemistry and Physics*, 9(10), 3425–3442. <https://doi.org/10.5194/acp-9-3425-2009>
- Dey, S., Di Girolamo, L., Van Donkelaar, A., Tripathi, S., Gupta, T., & Mohan, M. (2012). Variability of outdoor fine particulate (PM_{2.5}) concentration in the Indian subcontinent: A remote sensing approach. *Remote Sensing of Environment*, 127, 153–161. <https://doi.org/10.1016/j.rse.2012.08.021>
- Dolgorouky, C., Gros, V., Sarda-Esteve, R., Sinha, V., Williams, J., Marchand, N., et al. (2012). Total OH reactivity measurements in Paris during the 2010 MEGAPOLI winter campaign. <https://doi.org/10.5194/acp-12-9593-2012>
- Duan, J., Tan, J., Yang, L., Wu, S., & Hao, J. (2008). Concentration, sources and ozone formation potential of volatile organic compounds (VOCs) during ozone episode in Beijing. *Atmospheric Research*, 88(1), 25–35. <https://doi.org/10.1016/j.atmosres.2007.09.004>
- Evans, T. (2009). *Biological volatile organic compounds (BVOCs) emissions from the planktonic diatom Thalassiosira pseudonana*. The Graduate School, Stony Brook University: Stony Brook.
- Feng, Z., Marco, A. D., Anav, A., Gualtieri, M., Sicard, P., Tian, H., et al. (2019). Economic losses due to ozone impacts on human health, forest productivity and crop yield across China. *Environment International*, 131, 104966. <https://doi.org/10.1016/j.envint.2019.104966>
- Filella, I., & Penuelas, J. (2006). Daily, weekly, and seasonal time courses of VOC concentrations in a semi-urban area near Barcelona. *Atmospheric Environment*, 40(40), 7752–7769. <https://doi.org/10.1016/j.atmosenv.2006.08.002>
- Fleming, L. T., Weltman, R., Yadav, A., Edwards, R. D., Arora, N. K., Pillarisetti, A., et al. (2018). Emissions from village cookstoves in Haryana, India, and their potential impacts on air quality. *Atmospheric Chemistry and Physics*, 18(20), 15169–15182. <https://doi.org/10.5194/acp-18-15169-2018>
- Friedman, B., Link, M. F., Fulgham, S. R., Brophy, P., Galang, A., Brune, W. H., et al. (2017). Primary and secondary sources of gas-phase organic acids from diesel exhaust. *Environmental Science & Technology*, 51(18), 10872–10880. <https://doi.org/10.1021/acs.est.7b01169>
- García, J. P., Beyne-Masclat, S., Mouvier, G., & Masclat, P. (1992). Emissions of volatile organic compounds by coal-fired power stations. *Atmospheric Environment Part A: General Topics*, 26(9), 1589–1597. [https://doi.org/10.1016/0960-1686\(92\)90059-T](https://doi.org/10.1016/0960-1686(92)90059-T)
- Gilman, J. B., Kuster, W. C., Goldan, P. D., Herndon, S. C., Zahniser, M. S., Tucker, S. C., et al. (2009). Measurements of volatile organic compounds during the 2006 TexAQSGoMACCS campaign: Industrial influences, regional characteristics, and diurnal dependencies of the OH reactivity. *Journal of Geophysical Research: Atmospheres*, 114(D7). <https://doi.org/10.1029/2008JD011525>
- Goldberg, D. L., Vinciguerra, T. P., Anderson, D. C., Hembeck, L., Canty, T. P., Ehrman, S. H., et al. (2016). CAMx ozone source attribution in the eastern United States using guidance from observations during DISCOVER-AQ Maryland. *Geophysical Research Letters*, 43(5), 2249–2258. <https://doi.org/10.1002/2015gl067332>
- Goldstein, A. H., & Galbally, I. E. (2007). *Known and unexplored organic constituents in the earth's atmosphere*. <https://doi.org/10.1021/es072476p>
- Graus, M., Müller, M., & Hansel, A. (2010). High resolution PTR-TOF: Quantification and formula confirmation of VOC in real time. *Journal of the American Society for Mass Spectrometry*, 21(6), 1037–1044. <https://doi.org/10.1016/j.jasms.2010.02.006>
- Gu, Y., Li, Q., Wei, D., Gao, L., Tan, L., Su, G., et al. (2019). Emission characteristics of 99 NMVOCs in different seasonal days and the relationship with air quality parameters in Beijing, China. *Ecotoxicology and Environmental Safety*, 169, 797–806. <https://doi.org/10.1016/j.ecoenv.2018.11.091>
- Guenther, A., Jiang, X., Heald, C., Sakulyanontvittaya, T., Duhl, T., Emmons, L., & Wang, X. (2012). *The model of emissions of gases and aerosols from nature version 2.1 (MEGAN2.1): An extended and updated framework for modeling biogenic emissions*. <https://doi.org/10.5194/gmd-5-1471-2012>
- Guenther, A., Karl, T., Harley, P., Wiedinmyer, C., Palmer, P. I., & Geron, C. (2006). Estimates of global terrestrial isoprene emissions using MEGAN (model of emissions of gases and aerosols from nature). *Atmospheric Chemistry and Physics*, 6(11), 3181–3210. <https://doi.org/10.5194/acp-6-3181-2006>
- Gurjar, B., Ravindra, K., & Nagpure, A. S. (2016). Air pollution trends over Indian megacities and their local-to-global implications. *Atmospheric Environment*, 142, 475–495. <https://doi.org/10.1016/j.atmosenv.2016.06.030>
- Guttikunda, S. K., Goel, R., & Pant, P. (2014). Nature of air pollution, emission sources, and management in the Indian cities. *Atmospheric Environment*, 95, 501–510. <https://doi.org/10.1016/j.atmosenv.2014.07.006>
- Hakkim, H., Sinha, V., Chandra, B., Kumar, A., Mishra, A., Sinha, B., et al. (2019). Volatile organic compound measurements point to fog-induced biomass burning feedback to air quality in the megacity of Delhi. *The Science of the Total Environment*, 689, 295–304. <https://doi.org/10.1016/j.scitotenv.2019.06.438>
- Hallquist, M., Wenger, J. C., Baltensperger, U., Rudich, Y., Simpson, D., Claeys, M., et al. (2009). The formation, properties and impact of secondary organic aerosol: Current and emerging issues. *Atmospheric Chemistry and Physics*, 9(14), 5155–5236. <https://doi.org/10.5194/acp-9-5155-2009>
- Henze, D., Seinfeld, J., Ng, N., Kroll, J., Fu, T.-M., Jacob, D. J., & Heald, C. (2008). Global modeling of secondary organic aerosol formation from aromatic hydrocarbons: High- vs. low-yield pathways. *Atmospheric Chemistry and Physics*. <https://doi.org/10.5194/acp-8-2405-2008>
- Hersbach, H., Bell, B., Berrisford, P., Biavati, G., Horányi, A., Muñoz Sabater, J., et al. (2018). ERA5 hourly data on single levels from 1979 to present. *Copernicus Climate Change Service (C3S) Climate Data Store (CDS)* [Dataset]. <https://doi.org/10.24381/cds.adbb2d47>

- Hester, R. E., & Harrison, R. M. (1995). *Volatile organic compounds in the atmosphere*. Royal Society of Chemistry.
- Hewitt, C., Hayward, S., & Tani, A. (2003). The application of proton transfer reaction-mass spectrometry (PTR-MS) to the monitoring and analysis of volatile organic compounds in the atmosphere. *Journal of Environmental Monitoring*, 5(1), 1–7. <https://doi.org/10.1039/B204712H>
- Holzinger, R., Warneke, C., Hansel, A., Jordan, A., Lindinger, W., Scharffe, D. H., et al. (1999). Biomass burning as a source of formaldehyde, acetaldehyde, methanol, acetone, acetonitrile, and hydrogen cyanide. *Geophysical Research Letters*, 26(8), 1161–1164. <https://doi.org/10.1029/1999GL900156>
- Huangfu, Y., Yuan, B., Wang, S., Wu, C., He, X., Qi, J., et al. (2021). Revisiting acetonitrile as tracer of biomass burning in anthropogenic-influenced environments. *Geophysical Research Letters*, 48(11), e2020GL092322. <https://doi.org/10.1029/2020gl092322>
- IGOR, P. (2016). Wave metrics. Version 6.37, licensed [Software]. Retrieved from <https://www.wavemetrics.com/software/igor-pro-637-installer>
- Inomata, S., Tanimoto, H., Kato, S., Suthawaree, J., Kanaya, Y., Pochanart, P., et al. (2010). PTR-MS measurements of non-methane volatile organic compounds during an intensive field campaign at the summit of Mount Tai, China, in June 2006. *Atmospheric Chemistry and Physics*, 10(15), 7085. <https://doi.org/10.5194/acp-10-7085-2010>
- Jena, C., Ghude, S. D., Kumar, R., Debnath, S., Govardhan, G., Soni, V. K., et al. (2021). Performance of high resolution (400 m) PM_{2.5} forecast over Delhi. *Scientific Reports*, 11(1), 4104. <https://doi.org/10.1038/s41598-021-83467-8>
- Karl, T., Apel, E., Hodzic, A., Riemer, D., Blake, D., & Wiedinmyer, C. (2009). Emissions of volatile organic compounds inferred from airborne flux measurements over a megacity. *Atmospheric Chemistry and Physics*, 9(1), 271–285. <https://doi.org/10.5194/acp-9-271-2009>
- Karl, T., Striednig, M., Graus, M., Hammerle, A., & Wohlfahrt, G. (2018). Urban flux measurements reveal a large pool of oxygenated volatile organic compound emissions. *Proceedings of the National Academy of Sciences*, 115(6), 1186–1191. <https://doi.org/10.1073/pnas.1714715115>
- Karl, T. G., Christian, T. J., Yokelson, R. J., Artaxo, P., Hao, W. M., & Guenther, A. (2007). *The tropical forest and fire emissions experiment: Method evaluation of volatile organic compound emissions measured by PTR-MS, FTIR, and GC from tropical biomass burning*. Retrieved from <https://hal.archives-ouvertes.fr/hal-00296386>
- Kaskaoutis, D., Kumar, S., Sharma, D., Singh, R. P., Kharol, S., Sharma, M., et al. (2014). Effects of crop residue burning on aerosol properties, plume characteristics, and long-range transport over northern India. *Journal of Geophysical Research: Atmospheres*, 119(9), 5424–5444. <https://doi.org/10.1002/2013jd021357>
- Kleinman, L. I., Daum, P. H., Lee, Y., Nunnermacker, L. J., Springston, S. R., Weinstein-Lloyd, J., et al. (2003). Photochemical age determinations in the Phoenix metropolitan area. *Journal of Geophysical Research: Atmospheres*, 108(D3). <https://doi.org/10.1029/2002JD002621>
- Kumar, R., Ghude, S. D., Biswas, M., Jena, C., Alessandrini, S., Debnath, S., et al. (2020). Enhancing accuracy of air quality and temperature forecasts during paddy crop residue burning season in Delhi via chemical data assimilation. *Journal of Geophysical Research: Atmospheres*, 125(17), e2020JD033019. <https://doi.org/10.1029/2020JD033019>
- Kumar, R., Naja, M., Pfister, G. G., Barth, M. C., Wiedinmyer, C., & Brasseur, G. P. (2012). Simulations over South Asia using the Weather Research and Forecasting model with chemistry (WRF-Chem): Chemistry evaluation and initial results. *Geoscientific Model Development*, 5(3), 619–648. <https://doi.org/10.5194/gmd-5-619-2012>
- Langford, B., Misztal, P., Nemitz, E., Davison, B., Helfter, C., Pugh, T., et al. (2010). Fluxes and concentrations of volatile organic compounds from a South-East Asian tropical rainforest. *Atmospheric Chemistry and Physics*, 10(17). <https://doi.org/10.5194/acp-10-8391-2010>
- Legreid, G., Reimann, S., Steinbacher, M., Staehelin, J., Young, D., & Stemmler, K. (2007). Measurements of OVOCs and NMHCs in a Swiss highway tunnel for estimation of road transport emissions. *Environmental Science & Technology*, 41(20), 7060–7066. <https://doi.org/10.1021/es062309+>
- Lelieveld, J., Butler, T. M., Crowley, J. N., Dillon, T. J., Fischer, H., Ganzeveld, L., et al. (2008). Atmospheric oxidation capacity sustained by a tropical forest. *Nature*, 452, 737. <https://doi.org/10.1038/nature06870>
- Lelieveld, J., Gromov, S., Pozzer, A., & Taraborrelli, D. (2016). Global tropospheric hydroxyl distribution, budget and reactivity. *Atmospheric Chemistry and Physics*, 16(19), 12477–12493. <https://doi.org/10.5194/acp-16-12477-2016>
- Li, K., Li, J., Tong, S., Wang, W., Huang, R.-J., & Ge, M. (2019). Characteristics of wintertime VOCs in suburban and urban Beijing: Concentrations, emission ratios, and festival effects. *Atmospheric Chemistry and Physics*, 19(12), 8021–8036. <https://doi.org/10.5194/acp-19-8021-2019>
- Li, M., Zhang, Q., Streets, D., He, K., Cheng, Y., Emmons, L., et al. (2014). Mapping Asian anthropogenic emissions of non-methane volatile organic compounds to multiple chemical mechanisms. *Atmospheric Chemistry and Physics*, 14(11), 5617–5638. <https://doi.org/10.5194/acp-14-5617-2014>
- Li, P., Feng, Z., Catalayud, V., Yuan, X., Xu, Y., & Paoletti, E. (2017). A meta-analysis on growth, physiological, and biochemical responses of woody species to ground-level ozone highlights the role of plant functional types. *Plant, Cell and Environment*, 40(10), 2369–2380. <https://doi.org/10.1111/pce.13043>
- Liu, C., Ma, Z., Mu, Y., Liu, J., Zhang, C., Zhang, Y., et al. (2017). The levels, variation characteristics, and sources of atmospheric non-methane hydrocarbon compounds during wintertime in Beijing, China. *Atmospheric Chemistry and Physics*, 17(17), 10633. <https://doi.org/10.5194/acp-17-10633-2017>
- Liu, C., Zhang, C., Mu, Y., Liu, J., & Zhang, Y. (2017). Emission of volatile organic compounds from domestic coal stove with the actual alternation of flaming and smoldering combustion processes. *Environmental Pollution*, 221, 385–391. <https://doi.org/10.1016/j.envpol.2016.11.089>
- Liu, W., Wu, B., Bai, X., Liu, S., Lin, S., Luo, L., et al. (2019). *Study on the Emission Characteristics and Source Profiles of Volatile Organic Compounds for Typical Cement Plants in China* (Vol. 2019). Presented at the AGU Fall Meeting Abstracts A43M-2019
- Madronich, S. (2006). Chemical evolution of gaseous air pollutants down-wind of tropical megacities: Mexico City case study. *Atmospheric Environment*, 40(31), 6012–6018. <https://doi.org/10.1016/j.atmosenv.2005.08.047>
- Madronich, S., & Flocke, S. (1999). The role of solar radiation in atmospheric chemistry. In *Environmental Photochemistry* (Vols. 2/2L, pp. 1–26). Springer. https://doi.org/10.1007/978-3-540-69044-3_1
- Mahajan, A. S., De Smedt, I., Biswas, M. S., Ghude, S., Fadnavis, S., Roy, C., & Van Roozendael, M. (2015). Inter-annual variations in satellite observations of nitrogen dioxide and formaldehyde over India. *Atmospheric Environment*, 116, 194–201. <https://doi.org/10.1016/j.atmosenv.2015.06.004>
- Majumdar, D., Mukherjee, A., & Sen, S. (2011). BTEX in ambient air of a Metropolitan City. *Journal of Environmental Protection*, 2(01), 11. <https://doi.org/10.4236/jep.2011.21002>
- Mao, J., Ren, X., Brune, W. H., Olson, J., Crawford, J., Fried, A., et al. (2009). Airborne measurement of OH reactivity during INTEX-B. <https://doi.org/10.5194/acpd-8-14217-2008>
- MATLAB. (2019). MATLAB version 9.7 (R2019b), licensed [Software]. The MathWorks Inc. Received from <https://www.mathworks.com/>
- Mazuca, G. M., Ren, X., Loughner, C. P., Estes, M., Crawford, J. H., Pickering, K. E., et al. (2016). Ozone production and its sensitivity to NO_x and VOCs: Results from the DISCOVER-AQ field experiment, Houston 2013. *Atmospheric Chemistry and Physics*, 16(22), 14463–14474. <https://doi.org/10.5194/acp-16-14463-2016>

- McKeen, S., & Liu, S. (1993). Hydrocarbon ratios and photochemical history of air masses. *Geophysical Research Letters*, 20(21), 2363–2366. <https://doi.org/10.1029/93gl02527>
- Monks, P. S. (2005). Gas-phase radical chemistry in the troposphere. *Chemical Society Reviews*, 34(5), 376–395. <https://doi.org/10.1039/b307982c>
- Nakoudi, K., Giannakaki, E., Dandou, A., Tombrou, M., & Komppula, M. (2019). Planetary boundary layer height by means of lidar and numerical simulations over New Delhi, India. *Atmospheric Measurement Techniques*, 12, 2595–2610. <https://doi.org/10.5194/amt-12-2595-2019>
- Nelson, B. S., Stewart, G. J., Drysdale, W. S., Newland, M. J., Vaughan, A. R., Dunmore, R. E., et al. (2021). In situ ozone production is highly sensitive to volatile organic compounds in Delhi, India. *Atmospheric Chemistry and Physics*, 21(17), 13609–13630. <https://doi.org/10.5194/acp-21-13609-2021>
- Ohara, T., Akimoto, H., Kurokawa, J., Horii, N., Yamaji, K., Yan, X., & Hayasaka, T. (2007). An asian emission inventory of anthropogenic emission sources for the period 1980? 2020. <https://doi.org/10.5194/acp-7-4419-2007>
- Ojha, N., Naja, M., Singh, K., Sarangi, T., Kumar, R., Lal, S., et al. (2012). Variabilities in ozone at a semi-urban site in the Indo-Gangetic Plain region: Association with the meteorology and regional processes. *Journal of Geophysical Research: Atmospheres*, 117(D20). <https://doi.org/10.1029/2012JD017716>
- Ojha, N., Sharma, A., Kumar, M., Girach, I., Ansari, T. U., Sharma, S. K., et al. (2020). On the widespread enhancement in fine particulate matter across the Indo-Gangetic Plain towards winter. *Scientific Reports*, 10(1), 1–9. <https://doi.org/10.1038/s41598-020-62710-8>
- Pandey, A., Sadavarte, P., Rao, A. B., & Venkataraman, C. (2014). Trends in multi-pollutant emissions from a technology-linked inventory for India: II. Residential, agricultural and informal industry sectors. *Atmospheric Environment*, 99, 341–352. <https://doi.org/10.1016/j.atmosenv.2014.09.080>
- Parrish, D., Ryerson, T., Mellqvist, J., Johansson, J., Fried, A., Richter, D., et al. (2012). Primary and secondary sources of formaldehyde in urban atmospheres: Houston Texas region. *Atmospheric Chemistry and Physics*, 12(7), 3273–3288. <https://doi.org/10.5194/acp-12-3273-2012>
- Quigley, C. J., & Corsi, R. L. (1995). Emissions of VOCs from a municipal sewer. *Journal of the Air & Waste Management Association*, 45(5), 395–403. <https://doi.org/10.1080/10473289.1995.10467371>
- Rai, P., Furger, M., ElHaddad, I., Kumar, V., Wang, L., Singh, A., et al. (2020). Real-time measurement and source apportionment of elements in Delhi's atmosphere. *The Science of the Total Environment*, 742, 140332. <https://doi.org/10.1016/j.scitotenv.2020.140332>
- Ramachandra, T. (2009). Emissions from India's transport sector: Statewise synthesis. *Atmospheric Environment*, 43(34), 5510–5517. <https://doi.org/10.1016/j.atmosenv.2009.07.015>
- Robinson, A. L., Donahue, N. M., Shrivastava, M. K., Weitkamp, E. A., Sage, A. M., Grieshop, A. P., et al. (2007). Rethinking organic aerosols: Semivolatile emissions and photochemical aging. *Science*, 315(5816), 1259–1262. <https://doi.org/10.1126/science.1133061>
- Rogers, T., Grimsrud, E., Herndon, S., Jayne, J., Kolb, C. E., Allwine, E., et al. (2006). On-road measurements of volatile organic compounds in the Mexico City metropolitan area using proton transfer reaction mass spectrometry. *International Journal of Mass Spectrometry*, 252(1), 26–37. <https://doi.org/10.1016/j.ijms.2006.01.027>
- Sahay, S., & Ghosh, C. (2013). Monitoring variation in greenhouse gases concentration in urban environment of Delhi. *Environmental Monitoring and Assessment*, 185(1), 123–142. <https://doi.org/10.1007/s10661-012-2538-8>
- Sahu, L., Pal, D., Yadav, R., & Munkhtur, J. (2016). Aromatic VOCs at major road junctions of a metropolis in India: Measurements using TD-GC-FID and PTR-TOF-MS instruments. *Aerosol and Air Quality Research*, 16, 2405–2420. <https://doi.org/10.4209/aaqr.2015.11.0643>
- Sahu, L., & Saxena, P. (2015). High time and mass resolved PTR-TOF-MS measurements of VOCs at an urban site of India during winter: Role of anthropogenic, biomass burning, biogenic and photochemical sources. *Atmospheric Research*, 164, 84–94. <https://doi.org/10.1016/j.atmosres.2015.04.021>
- Sahu, L., Tripathi, N., Gupta, M., Singh, V., Yadav, R., & Patel, K. (2022). Impact of COVID-19 pandemic lockdown in ambient concentrations of aromatic volatile organic compounds in a metropolitan city of western India. *Journal of Geophysical Research: Atmospheres*, e2022JD036628. <https://doi.org/10.1029/2022jd036628>
- Sahu, L., Tripathi, N., & Yadav, R. (2017). Contribution of biogenic and photochemical sources to ambient VOCs during winter to summer transition at a semi-arid urban site in India. *Environmental Pollution*, 229, 595–606. <https://doi.org/10.1016/j.envpol.2017.06.091>
- Sahu, L., Tripathi, N., & Yadav, R. (2020). Observations of trace gases in Earth's lower atmosphere: Instrumentation and platform. *Current Science*, 118(12), 1893.
- Sahu, L., Yadav, R., & Pal, D. (2016). Source identification of VOCs at an urban site of western India: Effect of marathon events and anthropogenic emissions. *Journal of Geophysical Research: Atmospheres*, 121(5), 2416–2433. <https://doi.org/10.1002/2015JD024454>
- Sawyer, R. F., Harley, R. A., Cadle, S. H., Norbeck, J. M., Slott, R., & Bravo, H. (2000). Mobile sources critical review: 1998 NARSTO assessment. *Atmospheric Environment*, 34(12–14), 2161–2181. [https://doi.org/10.1016/s1352-2310\(99\)00463-x](https://doi.org/10.1016/s1352-2310(99)00463-x)
- Scott, P. S., Andrew, J. P., Bundy, B. A., Grimm, B. K., Hamann, M. A., Ketcherside, D. T., et al. (2020). Observations of volatile organic and sulfur compounds in ambient air and health risk assessment near a paper mill in rural Idaho, U.S.A. *Atmospheric Pollution Research*, 11(10), 1870–1881. <https://doi.org/10.1016/j.apr.2020.07.014>
- Seinfeld, J. H., & Pandis, S. N. (2016). *Atmospheric chemistry and physics: From air pollution to climate change*. John Wiley & Sons.
- Sen, A., Abdelmaksoud, A., Ahammed, Y. N., Banerjee, T., Bhat, M. A., Chatterjee, A., et al. (2017). Variations in particulate matter over Indo-Gangetic Plains and Indo-Himalayan Range during four field campaigns in winter monsoon and summer monsoon: Role of pollution pathways. *Atmospheric Environment*, 154, 200–224. <https://doi.org/10.1016/j.atmosenv.2016.12.054>
- Sharma, A., Ojha, N., Pozzer, A., Mar, K. A., Beig, G., Lelieveld, J., & Gunthe, S. S. (2017). WRF-Chem simulated surface ozone over south Asia during the pre-monsoon: Effects of emission inventories and chemical mechanisms. *Atmospheric Chemistry and Physics*, 17(23), 14393. <https://doi.org/10.5194/acp-17-14393-2017>
- Sheng, J., Zhao, D., Ding, D., Li, X., Huang, M., Gao, Y., et al. (2018). Characterizing the level, photochemical reactivity, emission, and source contribution of the volatile organic compounds based on PTR-TOF-MS during winter haze period in Beijing, China. *Atmospheric Research*, 212, 54–63. <https://doi.org/10.1016/j.atmosres.2018.05.005>
- SigSigmaPlot. (2018). SigmaPlot version 14, licensed [Software]. Systat Software Inc. Retrieved from <http://www.sigmaplot.co.uk/products/sigmaplot/>
- Sillman, S., Vautard, R., Menut, L., & Kley, D. (2003). O₃-NO_x-VOC sensitivity and NO_x-VOC indicators in Paris: Results from models and Atmospheric Pollution Over the Paris Area (ESQUIF) measurements. *Journal of Geophysical Research: Atmospheres*, 108(D17). <https://doi.org/10.1029/2002JD001561>
- Sindelarova, K., Granier, C., Bouarar, I., Guenther, A., Tilmes, S., Stavrou, T., et al. (2014). Global data set of biogenic VOC emissions calculated by the MEGAN model over the last 30 years. *Atmospheric Chemistry and Physics*, 14(17), 9317–9341. <https://doi.org/10.5194/acp-14-9317-2014>

- Sinha, V., Kumar, V., & Sarkar, C. (2014). Chemical composition of pre-monsoon air in the Indo-Gangetic Plain measured using a new air quality facility and PTR-MS: High surface ozone and strong influence of biomass burning. *Atmospheric Chemistry and Physics*, 14(12). <https://doi.org/10.5194/acp-14-5921-2014>
- Smith, D., & Španěl, P. (2005). Selected ion flow tube mass spectrometry (SIFT-MS) for on-line trace gas analysis. *Mass Spectrometry Reviews*, 24(5), 661–700. <https://doi.org/10.1002/mas.20033>
- Soni, M., Ojha, N., & Girach, I. (2021). Impact of COVID-19 lockdown on surface ozone build-up at an urban site in western India based on photochemical box modelling. *Current Science*, 120(2), 376. <https://doi.org/10.18520/cs/v120/i2/376-381>
- Srivastava, A., Soni, V., Singh, S., Kanawade, V., Singh, N., Tiwari, S., & Attri, S. (2014). An early South Asian dust storm during March 2012 and its impacts on Indian Himalayan foothills: A case study. *The Science of the Total Environment*, 493, 526–534. <https://doi.org/10.1016/j.scitotenv.2014.06.024>
- Steeghs, M., Bais, H. P., De Gouw, J., Goldan, P., Kuster, W., Northway, M., et al. (2004). Proton-transfer-reaction mass spectrometry as a new tool for real time analysis of root-secreted volatile organic compounds in Arabidopsis. *Plant Physiology*, 135(1), 47–58. <https://doi.org/10.1104/pp.104.038703>
- Stockwell, C., Veres, P., & Williams, J. (2015). Characterization of biomass burning emissions from cooking fires, peat, crop residue, and other fuels with high-resolution proton-transfer-reaction time-of-flight mass spectrometry. *Atmospheric Chemistry and Physics*, 15, 845. <https://doi.org/10.5194/acp-15-845-2015>
- Surl, L., Palmer, P. I., & González Abad, G. (2018). Which processes drive observed variations of HCHO columns over India? *Atmospheric Chemistry and Physics*, 18(7), 4549–4566. <https://doi.org/10.5194/acp-18-4549-2018>
- Tan, J.-H., Guo, S.-J., Ma, Y.-L., Yang, F.-M., He, K.-B., Yu, Y.-C., et al. (2012). Non-methane hydrocarbons and their ozone formation potentials in Foshan, China. *Aerosol and Air Quality Research*, 12(3), 387–398. <https://doi.org/10.4209/aaqr.2011.08.0127>
- Tang, X., Wang, Z., Zhu, J., Gbaguidi, A. E., Wu, Q., Li, J., & Zhu, T. (2010). Sensitivity of ozone to precursor emissions in urban Beijing with a Monte Carlo scheme. *Atmospheric Environment*, 44(31), 3833–3842. <https://doi.org/10.1016/j.atmosenv.2010.06.026>
- Thorenz, U. R., Baker, A. K., Elvidge, E. L., Sauvage, C., Riede, H., Van Velthoven, P. F., et al. (2017). Investigating African trace gas sources, vertical transport, and oxidation using IAGOS-CARIBIC measurements between Germany and South Africa between 2009 and 2011. *Atmospheric Environment*, 158, 11–26. <https://doi.org/10.1016/j.atmosenv.2017.03.021>
- Tong, X., Zhang, Z., Chen, X., & Shen, W. (2015). Analysis of volatile organic compounds in the ambient air of a paper mill – A case study. *Bioresources*, 10, 8487–8497. <https://doi.org/10.15376/biores.10.4.8487-8497>
- Tripathi, N., & Sahu, L. K. (2020). Emissions and atmospheric concentrations of α -pinene at an urban site of India: Role of changes in meteorology. *Chemosphere*, 127071. <https://doi.org/10.1016/j.chemosphere.2020.127071>
- Tripathi, N., Sahu, L. K., Wang, L., Vats, P., Soni, M., Kumar, P., et al. (2021). Characteristics of VOC composition at urban and suburban sites of New Delhi, India in winter. Figshare [Dataset]. <https://doi.org/10.6084/m9.figshare.12496169.v2>
- Valach, A., Langford, B., Nemitz, E., MacKenzie, A., & Hewitt, C. (2014). Concentrations of selected volatile organic compounds at kerbside and background sites in central London. *Atmospheric Environment*, 95, 456–467. <https://doi.org/10.1016/j.atmosenv.2014.06.052>
- Velasco, E., Lamb, B., Westberg, H., Allwine, E., Sosa, G., Arriaga-Colina, J., et al. (2007). *Distribution, magnitudes, reactivities, ratios and diurnal patterns of volatile organic compounds in the Valley of Mexico during the MCMA 2002 & 2003 field campaigns*.
- Wagner, P., & Kuttler, W. (2014). Biogenic and anthropogenic isoprene in the near-surface urban atmosphere — A case study in Essen, Germany. *The Science of the Total Environment*, 475, 104–115. <https://doi.org/10.1016/j.scitotenv.2013.12.026>
- Wang, L., Slowik, J. G., Tripathi, N., Bhattu, D., Rai, P., Kumar, V., et al. (2020). Source characterization of volatile organic compounds measured by proton-transfer-reaction time-of-flight mass spectrometers in Delhi, India. *Atmospheric Chemistry and Physics*, 20(16), 9753–9770. <https://doi.org/10.5194/acp-20-9753-2020>
- Wang, M., Shao, M., Chen, W., Yuan, B., Lu, S., Zhang, Q., et al. (2013). Validation of emission inventories by measurements of ambient volatile organic compounds in Beijing, China. *Atmospheric Chemistry and Physics Discussions*, 13(10). <https://doi.org/10.5194/acpd-13-26933-2013>
- Wang, W., Qi, J., Zhou, J., Yuan, B., Peng, Y., Wang, S., et al. (2021). The improved comparative reactivity method (ICRM): Measurements of OH reactivity under high-NO_x conditions in ambient air. *Atmospheric Measurement Techniques*, 14(3), 2285–2298. <https://doi.org/10.5194/amt-14-2285-2021>
- Warneke, C., De Gouw, J., Del Negro, L., Brioude, J., McKeen, S., Stark, H., et al. (2010). Biogenic emission measurement and inventories determination of biogenic emissions in the eastern United States and Texas and comparison with biogenic emission inventories. *Journal of Geophysical Research: Atmospheres*, 115(D7). <https://doi.org/10.1029/2009JD012445>
- Warneke, C., De Gouw, J. A., Edwards, P. M., Holloway, J. S., Gilman, J. B., Kuster, W. C., et al. (2013). Photochemical aging of volatile organic compounds in the Los Angeles basin: Weekday-weekend effect. *Journal of Geophysical Research: Atmospheres*, 118(10), 5018–5028. <https://doi.org/10.1002/jgrd.50423>
- Warneke, C., McKeen, S., De Gouw, J., Goldan, P., Kuster, W., Holloway, J., et al. (2007). Determination of urban volatile organic compound emission ratios and comparison with an emissions database. *Journal of Geophysical Research: Atmospheres*, 112(D10). <https://doi.org/10.1029/2006JD007930>
- Weather Underground. (2018). Weather History for Indira Gandhi International Airport, New Delhi for daily data [Dataset]. Received from <https://www.wunderground.com/history/daily/in/new-delhi/VIDP>
- WHO. (2017). *Review of evidence on health aspects of air pollution—REVIHAAP Project*.
- Williams, J., & Brune, W. (2015). A roadmap for OH reactivity research. *Atmospheric Environment*, 106, 371–372. <https://doi.org/10.1016/j.atmosenv.2015.02.017>
- Williams, J., Keßel, S. U., Nölscher, A. C., Yang, Y., Lee, Y., Yáñez-Serrano, A. M., et al. (2016). Opposite OH reactivity and ozone cycles in the Amazon rainforest and megacity Beijing: Subversion of biospheric oxidant control by anthropogenic emissions. *Atmospheric Environment*, 125, 112–118. <https://doi.org/10.1016/j.atmosenv.2015.11.007>
- Wu, C., Wang, C., Wang, S., Wang, W., Yuan, B., Qi, J., et al. (2020). Measurement report: Important contributions of oxygenated compounds to emissions and chemistry of volatile organic compounds in urban air. *Atmospheric Chemistry and Physics*, 20(23), 14769–14785. <https://doi.org/10.5194/acp-20-14769-2020>
- Wu, R., & Xie, S. (2018). Spatial distribution of secondary organic aerosol formation potential in China derived from speciated anthropogenic volatile organic compound emissions. *Environmental Science & Technology*, 52(15), 8146–8156. <https://doi.org/10.1021/acs.est.8b01269>
- Xue, L., Wang, T., Gao, J., Ding, A., Zhou, X., Blake, D., et al. (2013). Ozone production in four major cities of China: Sensitivity to ozone precursors and heterogeneous processes. *Atmospheric Chemistry and Physics Discussions*, 13(10), 27243–27285. <https://doi.org/10.5194/acpd-13-27243-2013>
- Yang, W.-B., Chen, W.-H., Yuan, C.-S., Yang, J.-C., & Zhao, Q.-L. (2012). Comparative assessments of VOC emission rates and associated health risks from wastewater treatment processes. *Journal of Environmental Monitoring: JEM*, 14, 2464–2474. <https://doi.org/10.1039/c2em30138e>

- Yang, Y., Shao, M., Wang, X., Nölscher, A. C., Kessel, S., Guenther, A., & Williams, J. (2016). Towards a quantitative understanding of total OH reactivity: A review. *Atmospheric Environment*, *134*, 147–161. <https://doi.org/10.1016/j.atmosenv.2016.03.010>
- Yuan, B., Hu, W., Shao, M., Wang, M., Chen, W. T., Lu, S., et al. (2013). VOC emissions, evolutions and contributions to SOA formation at a receptor site in eastern China. *Atmospheric Chemistry and Physics Discussions*, *13*(3), 6631–6679. <https://doi.org/10.5194/acp-13-8815-2013>
- Yuan, B., Shao, M., De Gouw, J., Parrish, D. D., Lu, S., Wang, M., et al. (2012). Volatile organic compounds (VOCs) in urban air: How chemistry affects the interpretation of positive matrix factorization (PMF) analysis. *Journal of Geophysical Research: Atmospheres*, *117*(D24). <https://doi.org/10.1029/2012JD018236>